DOE/NASA/12726-18
NASA TM-82940

NASA Redox Storage System Development Project

Calendar Year 1980

National Aeronautics and Space Administration
Lewis Research Center

December 1982

Prepared for
U.S. DEPARTMENT OF ENERGY
Conservation and Renewable Energy
Division of Energy Storage Systems

DOE/NASA/12726-18
NASA TM-82940

NASA Redox Storage System Development Project

Calendar Year 1980

National Aeronautics and Space Administration
Lewis Research Center
Cleveland, Ohio 44135

December 1982

Work performed for
U.S. DEPARTMENT OF ENERGY
Conservation and Renewable Energy
Division of Energy Storage Systems
Washington, D.C. 20545
Under Interagency Agreement DE-AI04-8AL12726

SUMMARY

The NASA Redox Storage System Development project is managed by the Redox Project Office of the Solar and Electrochemistry Division of the NASA Lewis Research Center in accordance with Interagency Agreement DE-AI04-80AL12726 (formerly DOE/NASA Agreement EC-77-A-31-1002). The Department of Energy (DOE) Headquarter's Office of Advanced Conservation Technologies has assigned lead center responsibility for this project to Sandia National Laboratories, Alburquerque, New Mexico, Storage Batteries Division of the Components and Standards Directorate (fig. 1).

This annual report (for the period ending approx Dec. 1980) was prepared as part of the reporting requirements under this interagency agreement. The report describes the technical accomplishments pertaining to the development of Redox systems and related technology. Task elements discussed in this report are representative of DOE policies in existence during calendar year 1980.

PROJECT BACKGROUND

The Energy Research and Development Agency (ERDA)-approved project development plan (PDP) entitled "Redox Flow Cell Development and Demonstration Project Plan" and dated December 14, 1974, describes a phased effort to develop and demonstrate a NASA-conceived Redox flow system. Sufficient energy storage capacity would be provided to supply useful operational experience and preliminary cost data as basic input for the design and construction of commercial systems.

Since this PDP was approved, the original schedules, areas of emphasis, and resource estimates have been modified several times to reflect available funding as well as shifts in pacing and priorities desired by ERDA/DOE program managers. The current project planning is based on a new multiyear project plan for development of Redox systems for solar applications and utility-load-leveling applications. The plan with schedular and funding modifications was endorsed by the lead center, Sandia National Laboratories, Albuquerque (SNLA) in July 1980.

The operating period preceding this report provided dramatic advances in the enabling technologies of ion-exchange membranes and electrocatalysts. Furthermore a series of novel, system-related concepts were added to the basic concept and their technical feasibility has been demonstrated.

The viability of the Redox concept has been demonstrated by the operation of short stacks of scaled-up Redox flow cells and by the operation of a 1-kW system. Project goals were met or exceeded with peak power densities greater than 75 W/ft^2 and roundtrip efficiencies of 75 percent on laboratory-size cells. All performance goals were exceeded in the laboratory-size (14.5 cm^2) cells. These accomplishments were made possible, in part, by optimizing the membranes for reduced resistivity and most significantly by developing electrocatalysts for the reduction and oxidation of chromium ions.

PROJECT OBJECTIVE AND DESCRIPTION

The overall objectives of the Government's battery storage program are to accelerate the development of reliable and economically viable electric energy storage systems and to enable the earliest possible commercialization of such systems.

The objectives of the NASA Redox Storage System Development project are to demonstrate the readiness of Redox system technology for solar-related and utility applications and to transfer Redox system technology to industry for product development and commercialization in order to meet the overall objectives of the Government's battery storage program.

The project's activities are accomplished principally through contracts with the private sector to provide early and effective transfer of technology. Government funds in support of this project are provided by DOE. Activities are coordinated with complementary projects and tasks being pursued by DOE. The technical project elements are described briefly in the following sections.

PROTOTYPE SYSTEMS DEVELOPMENT

This element provides for a major procurement to develop an industrial capability to take the current NASA Lewis technology and go on to the design, development, and commercialization of iron-chromium Redox storage systems. The procurement provides for a phased approach, beginning with multikilowatt Redox storage system development and testing and culminating with megawatt Redox storage systems for testing in the DOE-EPRI battery energy storage test (BEST) facility. This task also includes in-house system testing of a preprototype 1-kW system currently in operation.

APPLICATION ANALYSES

This element has as its primary purposes the definition of application concepts and technology requirements, specific system definition studies, and the identification of market sectors and their penetration potential. Included are the necessary component and system cost projections.

SUPPORTING TECHNOLOGY

This element includes both in-house and contractual efforts that encompass implementation of necessary technology improvements in membranes, electrodes, reactant processing, and system design.

PROJECT GOALS AND MAJOR ACCOMPLISHMENTS

The NASA Redox Storage System Development project schedule and milestones are shown in figure 2 for each of the project elements. The schedule includes the award of one or more multikilowatt Redox development contracts by November 1981 with the first preprototype 10-kW/80-kWh Redox system field

test completed by October 1983 at the Sandia National Laboratories photovoltaic advanced system test facility in Albuquerque, New Mexico. Completion of prototype field tests by June 1985, is planned with multikilowatt Redox technology readiness and technology transfer completed by December 1985. In parallel with these activities is the implementation of application analyses and the supporting technology tasks. Major accomplishments toward achieving these milestones are summarized here for each element.

PROJECT MANAGEMENT

The annual Redox project review was held for SNLA and the DOE Chicago Operations and Regional Office (CORO) in April 1980. During 1980,[1] 18 Redox presentations and 5 papers were given to members of industry, government, and technical societies.

PROTOTYPE SYSTEMS DEVELOPMENT

To support implementation of a multiyear project for the development of Redox systems for both solar photovoltaic and utility-load-leveling applications, a two-day industrial briefing was held at NASA Lewis in July 1980 to describe the technical status and project objectives to about 75 representatives of 60 industrial firms.

A 1-kW preprototype Redox storage system was designed and built and is in operation as a test bed for evaluating the interaction of a complete, full-function, Redox system with a solar array field (NASA Lewis/DOE systems test facility). The versatility of the system permits evaluation of several control concepts.

A request for proposal (RFP) was completed for the design, test, and evaluation of multikilowatt and megawatt Redox systems by the private sector. The RFP is planned to be issued in March 1981.

APPLICATION ANALYSES

A Redox computer model was developed to permit the determination of minimum-cost Redox systems for a variety of input conditions.

A study of the institutional issues related to the commercialization and deployment of Redox systems was implemented.

A Redox system cost projection study was completed that, based on reasonable production quantities, indicates that Redox systems are very cost competitive with other storage systems.

A preliminary residential market penetration study is in progress to compare Redox systems and advanced lead-acid battery systems in residential applications.

---

[1]Unless otherwise specified, all years are calendar years.

SUPPORTING TECHNOLOGY

Significant progress was made at the component, subsystem, and system levels. Feasibility of Redox system operation with a photovoltaic array was demonstrated.

Membrane resistivity and selectivity were shown to be adequate for solar and stand-alone applications.

Membrane resistivity was reduced from 7.0 Ω-cm^2 (Sept. 1978) to the present level of 3.6 Ω-cm^2. A fuller understanding of the iron-fouling problem was achieved, and membranes with more stable resistivities were developed.

Electrode technology improved significantly. Present laboratory cells have reached 20 000 cycles with a performance loss of less than 5 percent.

Single-cell performance continues to improve. Present cells have achieved a current density of 43 A/ft^2 (30 A/ft^2 in Sept. 1978) at 0.9 V and 50 percent depth of discharge (DOD).

Testing of cells in short (five cell) stacks yielded watt-hour, round-trip efficiencies of 81 percent at 20 A/ft^2, coulombic efficiencies of 98 percent, and peak power of 60 W/ft^2.

PROJECT ELEMENT SUMMARIES

ELEMENT 1.0 - PROJECT MANAGEMENT

Background

Element 1.0 includes the necessary coordination, planning, and preparation associated with program reviews, workshops, multiyear plans, and annual operating plans for the project activities. Also included are the necessary management to implement the project and control of resources to ensure milestone achievement.

Approach

Primary results of program planning and management are contained in three documents: (1) the interagency agreement (IA); (2) the annual operating plan (AOP); and (3) monthly management information and control system (MICS) reports. Project status is reported in detail through periodic reviews held with DOE, SNLA, and NASA managements. An AOP is prepared each year that responds to the resource guidelines provided by DOE Headquarters through the lead center (SNLA) to the Redox project manager. The AOP details the specific tasks to be performed along with the required resources. Reviews, workshops, and briefings are planned and implemented as required to support the project goals. Figure 3 displays the major milestones associated with this activity.

Status

As of December 1980, agreement on multiyear plan and resources was established with SNLA and CORO to include solar and utility-load-leveling system development.

During 1980, 18 Redox presentations and 5 papers were given to members of industry, government, and technical societies.

The annual project review was held for SNLA and DOE in April 1980.

A NASA Lewis industrial briefing was held in July 1980 to describe the Redox technical status and project objectives to about 75 representatives of 60 industrial firms.

A 1981 AOP was prepared.

ELEMENT 2.0 - PROTOTYPE SYSTEMS DEVELOPMENT

Background

The recent advances made in membrane technology and chromium electrode catalysis (discussed in following sections) have brought the Redox system concept to a level of development sufficient for implementation in complete operating systems.

Approach

Two parallel system development efforts were begun early in 1980. The first was to produce at Lewis a preprototype 1-kW system, complete with controls and instrumentation, in order to demonstrate and evaluate performance, interface interactions, loss mechanisms, adequacy of design approach, etc. This system was designed to operate as the storage system for a 5-kW (peak) solar photovoltaic array at Lewis. The second effort was to establish a contractual program to develop and produce larger Redox systems and to evalute them under credible operating conditions. A parallel aspect of the contractual effort is the development of a commercialization approach for the eventual marketing of Redox systems by the contractor. The first systems developed under contract will have power levels of about 10 kW, making them suitable for applications such as remote, stand-alone wind turbine or solar photovoltaic storage and grid-connected residential storage. An evolutionary development process will result ultimately in a 1-MW system, a size that is on the threshold of requirements for electric utility storage service.

Status

Multikilowatt Systems Development

During 1980, the statement of work defining the scope of the contractual effort to develop and evaluate Redox systems was prepared. Source Evaluation Board procedures were begun in late 1980 to put together a complete procurement package. The request for proposal is scheduled for release in March 1981.

Important inputs to the preparation of the procurement package resulted from an industrial briefing held at NASA Lewis on July 8-9, 1980. Invited to this briefing were all companies that might have an interest in the Redox system as a business opportunity. Approximately 75 representatives from 60 companies attended. These representatives were given, in great detail, the present Redox state of the art and projections for system costs and for expected technology advances. Also presented were the structure and the goals of the anticipated contractual effort. The companies represented at the industrial briefing ranged in size from the very small to the very large. The comments, questions, and concerns of the attendees were of great value during the subsequent preparation of the Redox procurement package.

This procurement is to initiate a phased approach to achieving the transfer of Redox technology to industry and eventual commercialization by industry. To date, the only industrial involvement with the NASA Lewis Redox project has been developmental research on membranes and electrodes by Ionics, Inc., and Giner, Inc., respectively, and the supply of graphite and carbon bipolar plates by several companies.

Phase I of this procurement will encompass the design, fabrication, and testing of two multikilowatt preprototype systems; the preparation of a multikilowatt commercialization plan; a conceptual megawatt Redox system design; and the conceptual design of a 100-kW submodule as the basic element of the megawatt system. On the basis of the results of the Phase I activities, a decision will be made whether or not to initiate Phase II and one or more contractors will be selected to continue with Phase II. Figure 4 presents the major milestones and schedule relating to Redox system production and testing for both phases of the contract program as planned in 1980. Phase II will encompass the design, fabrication, and test of prototype multikilowatt systems; the design, fabrication, and test of preprototype 100-kW submodules; the design and fabrication of a megawatt system for test in the BEST facility; a commercialization plan for megawatt Redox systems; and a commercialization approach for the multikilowatt Redox system.

The actual production of systems sized up to the 1-MW level will provide manufacturing cost data that will permit much more precise forecasts of the costs of Redox storage. The testing of these systems in realistic environments will prove the technical and economic viability of Redox storage and provide the operating experience needed for further system improvement.

The contract is planned to be a 52-month effort. This includes 28 months to complete Phase I and 24 months to complete Phase II. Phase II, however, is optional and its implementation will depend on achieving a successful Phase I activity based on the following criteria:

(1) Performance of the 10-kW Redox system
(2) Multikilowatt Redox commercialization plan
(3) Megawatt Redox storage system conceptual design
(4) 100-kW Redox module design for megawatt system applications
(5) Project management
(6) Phase II project development plan

Figure 5 shows the task sequence for the total program.

Lewis 1-kW Preprototype System

The nominal design specifications for the 1-kW Redox system assembled at NASA Lewis are presented in table 1. The 120-V dc voltage level was selected to minimize I^2R losses. The decision to group the single cells into four stacks was based partly on a consideration of shunt-current losses (intrastack losses tend to increase with the square of the number of cells in a stack) and partly on the fact that 39-cell stacks represent a reasonable step up from the previous maximum number of cells in a stack, 14. The system capacity of 13 kWh (700 liters of each reactant) was an arbitrary choice based on convenience. For tests actually run in 1980 the volume of reactants used was only about one-fourth of this design capacity to minimize cycle time. The depth of discharge range and the nominal current density were selected to avoid excessive pumping and cell I^2R losses. The cell size of 320-cm^2 active area was picked because necessary equipment and material were already on hand.

The voltage level of 120 V dc presented one system design problem: only 28-V dc pumps, controls, and instruments were readily available, and the lead times necessary to acquire 120-V equipment were not acceptable. It was therefore decided to use the 28-V dc equipment and to hard wire the 28-V pumps across a 24-cell section at the high-voltage end of the Redox system (fig. 6). Because of the variation of the voltage across these cells as the state of charge of the system changes, the pumping rates will be greatest when low flow rates are acceptable, and lowest when high rates are needed. Either situation results in system inefficiencies when using pumps designed for a single operating point. It was realized that the 28-V meter relays, flowmeters, and ampere-hour integrators could not tolerate the voltage changes inherent in direct connection to the Redox stacks. It was therefore necessary to install a 120-V/28-V dc-dc converter across the system 120-V dc bus. A system redesign would incorporate 120-V equipment.

The Redox system is designed so that, of the total of 156 single cells, 60 are separated into 10 six-cell trim packages. Through the use of meter relays, these trim packages are sequentially switched into or out of the load circuit to keep the bus voltage at 120 V dc.

The photovoltaic array consists of twenty-two 120 V strings of solar cells, which are also switched in and out to keep the array bus at 120 V dc, if possible, under existing load and insolation conditions. Trim cell switching is inhibited until all array strings are active, thus avoiding interactions between the two sets of controls. The array can be directly connected across the first 96 cells of the Redox system as shown in figure 7 (configuration 1) or directly across the system load in parallel with the active Redox cells (configuration 2).

As the four 39-cell stacks were assembled and tested individually, it was found that they all generated excessive amounts of hydrogen from their respective chromium electrodes. Since this gassing occurred even during discharge and at relatively low states of charge, it was evident that the problem was related to the chromium electrode catalyst. Analytical techniques revealed that the new batch of carbon felt from which these electrodes were produced did not accept the catalyst as had the previous batch. It was decided to proceed with the installation of these stacks in

the system, in spite of the gassing problem, in order to check out the system design concept and controls and to gain some operating experience. These goals were accomplished in spite of the operational difficulties. In addition, some charge-acceptance and polarization data out to the design power level were acquired, and the system was operated briefly in conjunction with the 5-kW (peak) solar photovoltaic array. Nonetheless, the five-cell stack of rebalance cells was unable to keep up with the system gas evolution rate, so the two reactants were always chemically out of balance. Therefore it was decided to completely rebuild the four stacks, taking advantage of a technique newly developed by Giner, Inc., for effectively catalyzing carbon felt for chromium electrodes. Laboratory tests had shown such electrodes to generate hydrogen in very modest amounts. This period would also be used to redesign and rebuild the five-cell rebalance stack.

As each of the four stacks was rebuilt, it was checked out individually. As expected, the hydrogen evolution rates had become almost negligible. The average resistance of stack cells, about 12 m Ω, compared well with laboratory results. However, the shunt-current power losses, as indicated by the steady-state current (taper current) attained while charging at a fixed voltage, were about twice as large as calculated. Most of this discrepancy has been shown to result from shunt paths unaccounted for in the mathematical model. These paths are effectively eliminated by using a polyethylene gasket to prevent the flowing fluids in the port slots (fig. 8) from contacting the membranes. Table 2 shows, for five-cell stacks, the history of shunt loss reduction as cells have been made to conform more closely to the model. In this table the cell configuration resulting in a 28-mA taper current is the same as in the 1-kW system. The insertion of the polyethylene gaskets reduced taper current to 12 mA. It can be inferred from these data that a reduction in shunt loss of about 50 percent would result from this simple modification to the cells of the 1-kW system.

The reassembled 1-kW system is shown in figure 9. Testing began in mid-November 1980. The initial work, whose focus was to characterize the performance of the Redox system, consisted of polarization tests, charge-discharge cycles, and performance-versus-flow-rate measurements (flow mapping). In these evaluations, all 156 cells were active and system charging was done with a dc power supply. Also, for the reasons mentioned earlier, power supplies were used to power the pumps, instruments, and controls.

Figure 10 presents the polarization curves for the 156-cell Redox system, taken at three different states of charge and presented in terms of average cell voltage versus current density. The dip in the discharge curve for the lowest state of charge (SOC) occurred when the weaker cells of the system fell off in performance. The voltage of such cells tends to drop to near zero and then stabilize. The rise in the charging curve for the highest state of charge was accompanied by the onset of a considerable increase in the hydrogen evolution rate, which is typical for higher charging voltages. The linear segments of the discharge curves have a slope equivalent to 15 m Ω/cell, about 25 percent greater than measured when the stacks were tested individually. It was determined that this rise in cell resistance resulted from the inability of the heating system in the shed housing the 1-kW system to keep the reactant temperature above 50° F in midwinter. Prior tests had been performed at a controlled 70° F. This temperature-induced increase in cell resistance results in a decrease in system energy efficiency.

Charge-discharge cycles were performed at nominal current densities of 30, 38, and 45 mA/cm^2. The system, initially fully discharged, was charged at the desired rate until the charging voltage reached 187 V (1.20 V/cell); then the current was allowed to taper off until a quasi-steady state of charge was attained. Discharge followed immediately and continued until complete. Typical data are shown in figure 11 in which state of charge, as indicated by the voltage of the open-circuit cell, is plotted against watt-hours of capacity for both charge and discharge. For a cycle between the reasonable open-circuit voltage limits of 0.94 and 1.15 V, the energy efficiency was 56.7 percent. Similar data for ampere-hours of capacity show a coulombic efficiency of 83.9 percent. The contributors to these relatively low efficiencies were the greater-than-expected average cell resistance and the higher-than-calculated shunt-current losses. As suggested in the preceding, both of these loss mechanisms can be easily and significantly reduced.

Flow mapping tests were also performed. In these tests the reactant flow rates were varied during a charge-discharge cycle to determine, at various states of charge, what flows were necessary to sustain system performance. It was found that flow rates three times greater than the stoichiometric requirement (i.e., the ideal, minimum flow for a given current and state of charge) were adequate to prevent any cells from falling to below zero voltage during discharge or rising unacceptably during charge. Tests on single cells have shown that 1.5 times the stoichiometric flow rate is sufficient for good performance, so the fact that the 156-cell system requires twice this rate indicates that some cells are getting only about one-half their share of the total flow. This problem relates to the difficulty in maintaining assembly tolerances when producing many cells by hand.

Table 3 presents the nominal loss rates for the various loss mechanisms for the 1-kW system. The present pumping loss rate relates to the worst-case situation: three times the stoichiometric flow rate called for by the design gross current density and the maximum design depth of discharge (80 percent). Better control over cell assembly tolerances would assure that all cells receive their proportionate share of the total flow and would thus permit operation closer to the 1.5 stoichiometric flow multiple shown to be sufficient for single cells. Pumps having an electric-to-hydraulic efficiency greater than the present 15 percent also would greatly reduce pumping losses. However, for very small systems such as this, low pump efficiency is a fact of life unless the pumps are specially designed for the specific application. Finally, use of an efficient pump speed control and solid-state logic devices would permit varying the pump speed as a function of the system state of charge instead of operating at the fixed, high speed required for the worst-case situation. Over a complete cycle this capability would greatly reduce the total energy required for pumping.

As mentioned earlier, a simple cell design change can be expected to reduce the intrastack shunt losses by about 50 percent. In addition, in light of the preceding discussion, operation at lower flow rates will permit the narrowing of the flow port slots in each cell at the expense of only modest pumping losses. Within certain limits the intrastack shunt losses are directly proportional to these flow port widths (resistances). In a like manner, interstack losses can be reduced by increasing the length or

reducing the diameter of piping between stacks. Finally a computational process can be used to determine the number of stacks, the number of cells per stack, and the size of piping connecting stacks to minimize the sum of intra- and interstack shunt losses and pumping requirements.

The power requirement indicated in table 3 for instrumentation and controls is specifically needed for the meter relays and associated contactors for trim cell control and for several integrating ampere-hour meters. The latter, being research devices, should not have their energy needs charged to the system. The former can be replaced by solid-state switching devices, which will considerably reduce their power demands.

Finally, although not tabulated in table 3, the I^2R losses could be reduced 20 percent by raising the system temperature 20 degrees F, to 70° F.

Note that the pump and shunt loss powers presented in table 3 are maximum rates. If the pump speeds were varied continuously in order to keep the flow rates at a constant multiple of the instantaneous stoichiometric flow rates as the system state of charge changed, the average pump power during a complete cycle would be much less than the indicated value. Similarly, the listed shunt loss rate is for the case of charging at the maximum rate (i.e., when the system voltage is at its highest). Since the shunt losses tend to vary between the second and third power of the system voltage, the integrated average shunt loss during a cycle would be considerably less than represented.

The final test performed with the 1-kW preprototype system in 1980 was the brief combined operation of the Redox and photovoltaic systems. Data from a typical run are presented in table 4. The two systems were operating in configuration 1, in which the photovoltaic array is connected directly across the first 96 cells of the Redox system. For the existing test conditions of load, Redox state of charge, and solar insolation, the array was fully activated (all 22 solar cell strings functioning) but was unable to reach the 120-V dc operating level. Therefore two trim cell packages (12 cells) were automatically brought into the circuit to boost the array output voltage from 111.5 V to 120.5 V for the load bus. Because of the relatively low Redox system state of charge of 33 percent, the array was capable, even at its 111.5-V output voltage, of providing charge to the Redox system through the 96-cell main stack. Thus the Redox system was expending 167 W through its trim cells to boost the array power to the load by 9 V and was at the same time accepting 1171 W of charge. During these tests the pumps, instruments, and controls were still being powered by separate power supplies. All controls and switching devices operated normally.

In summary, the 1-kW Redox preprototype system, although having been operational for only a short time in 1980, had already provided much valuable information. Control concepts have been shown to be valid and trouble free. Some insight has been gained into interactions at the mutual interfaces of the Redox system, the photovoltaic array, the load, and the control devices. Quantitative measurements of loss mechanisms have given direction for stack and system design changes to minimize these losses.

Figure 12 displays the major milestones associated with this activity.

ELEMENT 3.0 - APPLICATION ANALYSES

Background

An essential function related to the implementation of Redox system technology transfer and product development is application and market analyses. Included is the identification and definition of potential energy storage applications, the definition of technology requirements, appropriate system definition studies, and the identification of appropriate market sectors. This element supports these activities.

Approach

Specific activities are in progress or planned to provide conceptual designs of Redox storage system applications in sufficient depth to identify operational characteristics and to permit credible application cost projections. Institutional issues related to Redox system deployment and technology transfer are being addressed. Redox storage system conceptual production designs have been established to estimate production cost and to determine the influence of various parameters on production cost.

Status

The activity schedule (fig. 13) displays the specific tasks that support element 3.0. Each task area is discussed here.

Redox System Cost Projections - United Technologies Corp.

The cost projections addressed in this task are directed at selling price and application costs. United Technologies Corp. has been under contract (DEN3-126) to provide an estimate of projected manufacturer's selling price of two different Redox system sizes based on a reasonable production level. This effort is discussed here. A second task is planned to begin in early 1982 to provide costs of Redox applications based on detailed application concepts. This second task will use data generated by application concept studies to be performed beginning late in 1981. The application concepts will be generated for selected residential, commercial, and solar stand-alone applications.

The objectives of the contract with United Technologies Corp. were to establish Redox storage system conceptual production designs, to estimate production cost, and to determine the influence of various parameters on production cost. The results of the study are for the following cases:

(1) 10-kW/500-kWh Redox systems at an annual production rate of 1000 units
(2) 10-MW/100-MWh Redox systems at an annual producton rate of 100 units

Estimated manufacturer's selling price includes taxes, plant costs, depreciation, etc.

Significant conclusions drawn from the study show that the Redox cell and stack are amenable to mass production techniques with a relatively low material cost. For both system size requirements the cell and stack cost is a relatively minor factor in the total estimated cost. In both cases the system cost is dominated by the cost of the reactants and associated tankage (i.e., 79 to 87 percent of the cost of the 10-kW/500-kWh system and 56 to 71 percent of the cost of the 10-MW/100-MWh system).

Estimates of the manufacturer's selling price for the 10-kW/500-kWh system with an annual production rate of 1000 units are shown in table 5. The range reflects the chromic reactant cost range from $0.32/lb to $1.30/lb. Reactant concentration is 1 molar.

Estimates of the manufacturer's selling price for the 10-MW/100-MWh system with an annual production rate of 100 units are shown in table 6. Reactant concentration is 2 molar.

Lower costs for the megawatt systems are largely due to a current density of 100 A/ft^2, as opposed to 50 A/ft^2 for the kilowatt systems, and a much higher production volume of components for the megawatt systems as well as a 2 molar reactant concentration.

Market Analyses

The analyses addressed in this task are directed toward identifying favorable market sectors and their potential for penetration by Redox storage systems. Such data provide a focus for the appropriate system size and the requirements for Redox design and development. They identify those market segments favorably influenced by existing or planned energy legislation and thus provide direction for information dissemination and possible field test sites to enhance the introduction of Redox systems to potential users.

Earl Warren Legal Institute (Grant NAG3-111). - The object of this study is to identify those institutional issues related to Redox system deployment and technology transfer. The study is currently in progress and preliminary data indicate that the existing legislation, such as the National Energy Conservation Policy Act (NECPA) and the Public Utilities Regulatory Policy Act (PURPA), may have an important bearing on the commercial uses of Redox. The NECPA may provide direct grants for certain user classes; these grants could provide an early stimulus for Redox applications. It appears that certain small power producers may offer a special opportunity for Redox applications. Data collection and evaluation remain to be completed before conclusions can be drawn.

Aerospace Corporation (NASA-AF Interagency Order C-42701-D). - This study is directed toward performing a preliminary assessment of the market penetration potential for residential Redox system applications. The approach is to perform a financial analysis of a Redox system in a favorable residential application and to compare it with financial analyses of grid-only and advanced lead-acid battery storage, in all cases with and without photovoltaics. The study has not yet been completed; however, some preliminary results are available and are reported here. Table 7 indicates some of the study assumptions and table 8 summarizes the results. Note that

this study was intended only as an initial investigation to determine if a thorough market penetration study was warranted. As such, this study was based on several arbitrary assumptions and was limited in scope.

ELEMENT 4.0 - SUPPORTING TECHNOLOGY

Membrane Development

Background

Membranes used in Redox flow cells consist of ion-exchange resins that are fabricated into thin sheets reinforced by a thin layer of woven fabric. The resin, at present, is a copolymer of vinylbenzyl chloride and dimethylaminoethyl methacrylate, which form the crosslink and backbone components, respectively. The following parameters determine the properties of ion-exchange membranes:

(1) Backbone monomer type
(2) Crosslink monomer density and type
(3) Fraction of nonpolymerizable material (NP content) in the membrane precursor
(4) Amount of polymerizing catalyst (catalyst level)
(5) Total membrane thickness (different substrate backing or backing processing)
(6) Amount of functionality (addition of functional groups and sites to polymer structure)

By incorporating variations into these parameters, a wide selection of membrane characteristics is possible. The membranes are given an ion-exchange character to take advantage of Donnan exclusion and to prohibit cations from passing through the membrane by having cation charge sites incorporated into its structure. The more numerous these sites, the more selective the membrane would be. To further exclude cation passage, the effective pore size must be as small as posible, yet not hinder the passage of anions. (Because of the very small size of the hydrogen ion, it is impossible to prevent its passage through the membrane.) A membrane's success in excluding cation passage is referred to as its "selectivity." The selectivity and the conductivity of a membrane are of great importance. Consequently efforts to optimize the membrane are evaluated by measuring both factors.

The density of charge sites that are incorporated within the membrane structure is measured in terms of its ion-exchange capacity (IEC) in milliequivalents per dry gram of material (meq/dry g). In more recent membranes only a very thin layer of resin is required to accomplish the exclusion of ions, allowing a reduction in substrate thickness and a slight reduction in resistance to anion passage. The membrane engineering that is applied to adjust pore size is not well understood but is affected by polymerization conditions, including such things as the solvent used and the NP content.

Contained in the following sections are highlights of contract work performed, results of contract and in-house testing programs, and conclusions to be drawn from these evalutions.

Ionics, Inc.

Approach. - The membrane development program, which began in 1974 at Ionics, Inc., is presently in its fifth follow-on phase, begun in December 1980 (contract DEN3-204). Highlighted in this report will be the 1980 work (contract DEN3-137). During this reporting period (July 1979 to Nov. 1980; DEN3-137) progress was made in optimizing the CDIL chemistry formulation, a copolymer of vinylbenzyl chloride (VBC) and dimethylaminoethyl methacrylate, (DMAEMA), for area resistivity and selectivity and in improving fabrication techniques in order to improve yield and progress to larger membranes. Membrane samples were fabricated by incorporating variations in the membrane parameters (crosslink type and density, catalyst level, nonpolymerizable fraction, functional group addition, and reduction of total membrane thickness). Promising samples were then sent to Lewis for in-house analysis.

Status. - Table 9 is an example of typical characterization data gathered on each membrane sample. In addition to acquiring characterization data, iron fouling and permeability tests are also performed. Table 10 is an example of this type of data. Table 11 is a summary table of the information gathered from experiments involving variation of catalyst content. Membranes with a low catalyst content of 0.0625 percent have lower cell resistivities and good selectivities. The present "standard membrane" incorporates this variation. Other characteristics of the standard membrane are an NP content of 27.5 percent and a selectivity of 20 $\mu gFe/h/cm^2/moles/liter$. Resistance stability is much greater than in the past standard membrane, which had a catalyst content of 0.5 percent. A complete review of the recent contractual efforts on these membrane variations can be found in the contractor's latest report (ref. 1). Additional information on past efforts in this area by the same contractor can be found in previous reports (refs. 2 to 4).

Lewis Research Center - Membrane evaluation

Approach. - The in-house work done in the membrane area deals primarily with evaluation of membranes that are produced as a result of the Ionics, Inc., contracts. Selected membranes that have undergone tests at Ionics are sent for evaluation and screening tests at Lewis. These tests consist of

(1) Dye testing for pinholes: Pinholes allow solution crossmixing and therefore a reduction in storage capacity.
(2) Static diffusion for selectivity: Small membrane samples are placed between two half-cells containing chambers filled with various solutions and exposed to various temperature conditions. Periodically, a sample of solution is withdrawn and analyzed. Selectivity is then determined.
(3) Area resistivity: Resistivity is determined in various solutions at various temperatures. These measurements are made under static (nonflow) conditions.
(4) Resistivity flow tests: Resistivity is determined in various solutions under flow conditions.

(5) Redox cell performance: Performance is determined during charge and discharge at several reactant and acid concentrations and operating temperatures. Solution crossmixing and variation of resistance with time are also monitored.

In addition to these routine tests, membrane surface fouling measurements are made on selected samples. In these tests the area resistivity of each of several membrane samples is measured after presoaking in solutions containing various concentration ratios of $FeCl_3$ to $FeCl_2$ in 2.0 N HCl. Resistances are measured with an ac bridge at 1000 Hz. Data are normalized by subtracting the resistance of the cell without a membrane.

Additional information on screening tests and apparatuses involved can be found in references 5 and 6.

Status. - Results of resistivity flow tests on various membrane formulations are presented in table 12. Included in this table are preliminary results of new thinner fabric-backed membranes produced during the present contract (DEN3-204). In general, 0.5 M ferric iron solutions have a minimal effect on membrane "fouling." Large resistance increases occur between 1.0 M and 1.5 M ferric iron concentrations. Among membranes with acceptable selectivity, the new standard membrane formulations foul the least at ferric ion concentrations above 0.5 M. The enhanced conductivity imparted by 2.0 N HCl is almost balanced by the increased fouling tendency caused by the higher chloride ion content. Results shown are for samples from each type of variation that was fabricated at Ionics, Inc.

Membranes that perform well in selectivity and resistivity screening tests are run in small (14.5 cm^2) laboratory-size Redox cells. Results of performance data are shown in figure 14. The data are obtained by measuring cell voltage at various current densities during charge and discharge. These polarization curves were taken at 50 percent depth of discharge. It is interesting to note that the curves for the new standard membrane in 1.5 M solutions lie very close to the curves for the old standard membrane in 1.0 M solutions. The vertical distance between a charge and discharge curve indicates a measure of the cell voltage efficiency, and the slope of the discharge curve is the membrane resistance if there are no other significant polarizations or IR losses. The improvement in discharge current density at 0.9 V, between the two membranes, in 1.0 M solutions is about 43 percent.

A similar set of data was obtained for a cell with a new, thin fabric membrane. The results shown in figure 15 are compared with those for the new standard membrane. An improvement of about 16 percent is indicated. However, from table 12 it can be seen that the selectivity of the fabric C membrane is not as good as that of the new standard CD1L-AA5-0.0625. In addition, the fabric C membrane has slightly higher area resistivity in 1.5 M iron than does the new standard. Since it will be desirable in the near future to use 2.0 M solutions (to decrease tank size), the behavior in 1.5 M iron solutions becomes very important in deciding which membranes are superior. Selectivity is also a very important criterion. More samples of this thin membrane are being prepared to try to improve selectivity and make the membrane surface more resistant to fouling.

The effect on membrane resistivity of soaking in acidified iron solutions of various Fe^{+3}/Fe^{+2} ratios is presented in figure 16. The "fouling" effect is seen to be due to the presence of ferric ion. This fouling is most likely the result of an interaction between the positive charges within the membrane and the negatively charged chloro-complexes of the ferric ion. Fouling is a reversible phenomenon in that resistivity returns to the original value observed in 2.0 N HCl when a fouled membrane is resoaked in 2.0 N HCl.

Resistivity stability is determined by means of the resistivity flow test, which involves measurement of area resistivity as a function of time. Test durations are approximately 150 h. Most stable membranes exhibit an initial resistance increase and then level off within the prescribed period of time.

Complete data and results of tests performed on membrane samples, other than the new thin fabrics, are given in references 1 and 5.

An examination of data obtained from resistivity, selectivity, and performance tests indicates that the CD1L-AA5-0.0625 catalyst membrane is the best membrane to date for use in Redox energy storage systems. It is now being used as the standard membrane in Redox system tests, replacing the former standard CD1L-A5-0.5 catalyst membrane. Details are given in reference 5.

The new thinner membranes are promising with respect to area-resistivity reduction. Attempts are now being made to increase selectivity without changing the improved area resistivity.

Lewis Research Center - Membrane Modeling

Background. - As the Redox system cycles through charge and discharge, the volume of the reactant solution containing chromium has been observed to steadily increase over a period of time. For example, during a 3-week interval the transfer rate for a six-cell, 0.33-ft^2 stack (total membrane area, 2 ft^2) averaged 0.9 milliliter/h. An analysis was undertaken in order to identify the phenomena contributing to this solution transfer and to determine their relative significance. The theoretical approach, coupled with supporting experimental work, will provide a guide for the stabilization or elimination of solution transfer.

Approach. - Because the membrane is permeable to three species (H^+, Cl^-, and H_2O), transport can be described by using three flux equations. Expressed in terms of the measurable quantities of volume flux J_v, solvent flux J_s, and current I, the equations are

$$\left.\begin{aligned} J_v &= L_{11}\,(\Delta p - \Delta\pi) + L_{12}\,(\Delta\pi_s/C_s) + L_{13}E \\ J_s &= L_{21}\,(\Delta p - \Delta\pi) + L_{22}\,(\Delta\pi_s/C_s) + L_{23}E \\ I &= L_{31}\,(\Delta p - \Delta\pi) + L_{32}\,(\Delta\pi_s/C_s) + L_{33}E \end{aligned}\right\} \qquad (1)$$

where Δp is the hydrostatic pressure difference, $\Delta\pi$ is the osmotic pressure difference due to the impermeable species, $\Delta\pi_s$ is the osmotic pressure

difference due to the permeable species, C_s is the solute concentration, E is the applied field, and L_{ij} are the Onsager transport coefficients (ref. 7).

One can see that the magnitude and direction of the total volume flux (solvent and electrolyte) is a sum of several terms. The approach taken involves determining the relative contribution of each factor to transport. These factors are

(1) Hydrostatic pressure differences: Because the design of the Redox system is symmetric, the hydrostatic pressure differences were assumed to be small and are not considered here.

(2) Osmotic pressure differences: The osmotic pressure in dilute solutions is given by the relation

$$\pi = RT\Sigma C_j \qquad (2)$$

where C_j is the volume concentration of each solute, R is the gas constant, and T is temperature. Strictly speaking, this relation is only valid for infinitely dilute solutions, but it can be used to predict sign and order of magnitude of osmotic pressure differences. In the Redox system a number of different species may be present as a result of complexation (e.g., $[Cr(H_2O)_5Cl]^{+2}$, $[Cr(H_2O)_6]^{+3}$, H_3O^+, and Cl^- in discharged chromium solutions or $FeCl^{+2}$, $FeCl_3$, $FeCl_4^-$, Fe^{+3}, H_3O^+, and Cl^- in charged ferric ion solutions). In principle, if all equilibrium constants for complexation at a given temperature for a given system are known, the amounts of each species and hence the osmotic pressure differences between the two solutions can be calculated.

Experiments were run using reactant solutions 1.1 M $FeCl_2$, 1 N HCl/0.9 M $CrCl_3$, and 1.0 N HCl for a stack of cells that were allowed to charge and discharge repetitively. Although solution transfer was minimized initially, a net transfer always occurred to the chromium side, in contrast to the results obtained from static diffusion cell tests. Consequently other factors affecting volume flux were examined.

(3) Relative mobility differences: In the Redox system both ions of the HCl electrolyte are membrane permeable. The degree to which concentrations in each solution change during charge and discharge is governed by the anion, cation, and solvent transference numbers, where $t_+ = f(J_+/I)$(f is the Faraday constant, I is the current, and J_+ is the proton flux). The anionic transference number is $1 - t_+$ and t_{H_2O} is expressed as the number of moles of water transferred per faraday of electricity. Table 13 depicts how various factors are affected when the membrane transference numbers are varied for a sample calculation assuming continuously charging and discharging cells with 98 percent current efficiency. The solution volumes for iron and chromium solutions indicate a steadily increasing chromium solution volume. This effect results from the assumption of less than 100 percent current efficiency. The total ion concentration differences across the membrane, which are proportional osmotic pressure differences, are also given. Positive values indicate that the chromium solution has the higher osmotic pressure. This suggests a tendency for water to move to the chromium

solution and/or the electrolyte to move to the iron solution in order to achieve equilibrium. The relative mobilities of water and electrolyte determine the extent to which each moves (i.e., one can expect a higher water diffusion coefficient, which implies that the net result is greater water transport to the chromium ion solution). Similar results have been observed in silver-hydrogen batteries (ref. 8). Similar calculations, where the water moves to the iron solution (a more unusual situation), are shown in table 14. It is interesting to note that different combinations of transference numbers determine the direction of osmotic pressure gradient. Differences in hydrogen ion concentrations at the end of charge or discharge are also calculated, and the positive values indicate the tendency for electrolyte to diffuse to the iron solutions and water to diffuse to the chromium solutions.

The approximation used in calculating the values in tables 13 and 14 assumes constant transference numbers, and effects such as current efficiency, pressure differences, and concentration gradients are considered independently. A more realistic calculation uses a Nernst-Planck formalism modified to include convection:

$$\left.\begin{aligned} J_+ &= (C_{H+})(v) - (D_{H+})\left(\frac{\partial C_{H+}}{\partial x}\right) + (C_{H+})\left(\frac{\partial \Psi}{\partial x}\right) \\ J_- &= (C_{Cl^-})(v) - (D_{Cl^-})\left(\frac{\partial C_{Cl^-}}{\partial x}\right) - (C_{Cl^-})\left(\frac{\partial C}{\partial x}\right) \\ v &= d_h\left(RT\omega X\,\frac{\partial \Psi}{\partial x} - \frac{\partial p}{\partial x}\right) \end{aligned}\right\} \qquad (3)$$

where v is the volume flow, d_h is the hydrodynamic permeability, ωX is the membrane charge density, C_{H+} is the concentration of hydrogen ion, C_{Cl^-} is the concentration of chloride ion, D_{H+} is the hydrogen ion diffusion coefficient, D_{Cl^-} is the chloride ion diffusion coefficient, $\partial\Psi/\partial x$ is the potential gradient, and $\partial p/\partial x$ is the pressure gradient.

Integrated forms of these coupled differential equations derived by Schlog (ref. 9) assume the form

$$\left.\begin{aligned} J_+ &= \frac{v\omega X}{4}\;\frac{D_{H+} + D_{Cl^-}}{D_{Cl^-}}\;(1 + r)\;\;(1 + s) \\ J_- &= -\frac{v\omega X}{4}\;\frac{D_{H+} + D_{Cl^-}}{D_{H+}}\;(1 - r)\;\;(1 - s) \\ v &= \frac{D_o}{\delta}\left(\frac{\Delta p}{RTX} - \omega\Delta\Psi\right) \end{aligned}\right\} \qquad (4)$$

where δ is the membrane thickness, $\Delta\Psi$ is the potential difference, and D_o is the hydrodynamic diffusion coefficient.

The total current is given by $I = f(J_+ + J_-)$. For different values of total current, the solution parameters r and s can be calculated by numerical methods and, together with other parameter values such as applied pressure and applied field, allow the fluxes of the proton, chloride ion, and water to be calculated.

One can see that the total volume flux depends on membrane charge density and thickness. As those parameters change, the total volume flux will change.

Status. - Measurements were made with static diffusion cells to arrive at values of concentrations that would minimize the osmotic pressure difference between initially uncharged solutions. These results are shown in figure 18, where the ordinate represents a term proportional to the volume flux. For initially discharged solutions with 1.0 N HCl, osmotic equilibrium occurs somewhere between the combinations 1.0 M $FeCl_2$/1.0 M $CrCl_3$ and 1.2 M $FeCl_2$/0.8 M $CrCl_3$.

Summary. - The combination of salt and acid concentrations that gives isotonic solutions for initially discharged reactants has been determined experimentally. However, such solutions in a stack of cells being cycled do not prevent a net transfer of solvent to the chromium system. The foregoing analyses show that several factors can contribute to the phenomenon. Among these are the transport numbers for the ionic species and water, membrane charge density, thickness, and permeability, and diffusion coefficients. Additional experimentation plus further refinements in the analytical approach will be used to quantify the relative contributions of the various factors. This will direct the development effort for a technique to counter the fluid transfer. Figure 19 displays the major milestones associated with this activity.

Electrode Development

Giner, Inc.

Background. - Giner, Inc., performed screening studies of various Redox couples and electrode materials during 1975 and 1976 under contract NAS3-19760. Eight Redox couples were experimentally examined for electrochemical activity. The solubility, viscosity, and conductivity of their various aqueous solutions were also measured. Four of the most promising couples, including iron and chromium, were tested with various electrocatalysts. Four Redox cell designs were also investigated.

During 1977 and 1978, under contract NAS3-20794, additional work focused on the chemical and electrochemical properties of the chromic/chromous couple. The solubility and stability of chromous and chromic solutions were determined, and numerous electrocatalysts were experimentally investigated. Gold-lead combinations were identified in the spring of 1978 as providing electrochemically reversible surfaces for the chromium reduction and oxidation reactions.

Follow-on work was begun in 1979 under contract DEN3-97 to further develop the gold-lead catalyst system by specifying substrate materials and catalyst application methods. Other areas of investigation included alter-

native electrocatalysts and full-cell testing. Electrode performance changes as a result of the crossmixing of reactants through the membrane and the impurities found in technical-grade chromium chloride were also studied.

Work on the current contract (DEN3-198) began in mid-1980 with the primary objectives of characterization of the carbon/graphite felt substrate material; optimization of the gold-lead catalysis procedure; preparation of full-size, assembly-ready electrodes; and the study of alternative catalysts.

Approach. - Cyclic voltammetry was used to qualitatively and quantitatively evaluate various carbon and graphite felt substrate materials for electrochemical activity, with and without catalyst additions. Chromium oxidation and reduction, hydrogen ion reduction, and lead oxidation and reduction reactions were measured to characterize the electrodes.

Surface activity of the felt materials was modified through treatment in acid or base solutions in an attempt to "normalize" all of the felt lots prior to catalyst applications. Water absorption and retention properties of each felt were determined so that gold solutions could be added quantitatively. Several methods for gold application were evaluated for uniformity of gold distribution on the felts. Electrochemical activity as a function of gold loading was also investigated. Studies were made of bismuth and bismuth-gold catalyzed felts as alternative catalyst systems.

Status. - The research performed at Giner, Inc., disclosed significant variability among the lots of carbon felt received from the vendor. Some lots of felt had strong chemical reduction properties that affected the gold deposition onto the felt matrix. Treating this type of carbon felt with nitric acid changed the surface activity, giving better gold distribution and performance. Poor gold distribution generally results in a high hydrogen evolution rate and in a sudden change in discharge performance as the lead deplates and the electrode reverts to a less-active carbon surface.

A catalyst application method using an alcohol-gold solution was suggested. Alcohol greatly improved fiber wettability and resulted in a more homogeneous gold distribution. A joint patent disclosure was filed with NASA for this catalysis procedure. This procedure was used successfully to prepare the 156 chromium electrodes used in the NASA 1-kW Redox storage system.

Several other gold catalyst application methods were studied but did not appear to provide uniform gold distribution. A vacuum method was developed that used reduced pressure to remove air from the felt and give better wettability for the cleaning treatment and for adding the gold solution without the use of alcohol. Nonuniform gold distribution was evident with this procedure because gold migrated to the outer surface of the felt piece during the long drying period.

Four different lots of carbon and graphite felt, each catalyzed at four different gold loadings (3, 6, 12.5, and 25 $\mu g\ Au/cm^2$) were evaluated by cyclic voltammetry. The felts were treated in hot 1.0 N KOH and then activated by adding a methanol-gold solution, followed by thermal reduction of the gold salt to gold at 260° C. Cyclic voltammetry testing gave no strong, consistent correlation with gold loading. Graphite felt performance was generally lower than that of carbon felt.

Evaluation of bismuth and gold-bismuth as possible catalysts for the chromium electrode showed that electroplated bismuth on carbon felt has a high hydrogen overvoltage and definite activity for chromous oxidation and chromic reduction. This material will be further examined during 1981.

Summary. - The major issue in the chromium electrode development work is to consistently prepare electrodes with good electrochemical performance. Variations in carbon felt properties (lot to lot and within lot) appear to account for most of the variations in performance. Specific cleaning treatments and catalyzing procedures can generally be identified for each lot of carbon felt. However, a "normalization" step for all lots of felt has not been developed. A joint effort with a carbon felt manufacturer will be started to systematically identify a carbon felt fabrication procedure to manufacture a "Redox-grade" carbon felt.

Lewis Research Center - Electrode Preparation and Screening

Background. - Redox flow cell performance is largely determined by the electrochemical characteristics of the inert electrodes. The requirements for a reversible iron electrode have been met satisfactorily by using an uncatalyzed carbon felt. However, studies have shown that a lead-gold catalyst is needed for the chromium electrode to increase the rates of chromium reduction and oxidation and to provide a hydrogen evolution overpotential. (Thermodynamically hydrogen should be evolved before chromium is reduced.) Appreciable coevolution of hydrogen not only reduces the current efficiency of the system but, over a period of many cycles, also allows the system to become chemically out of balance and thus to lose effective capacity. The performance of these carbon felt electrodes depends on the production history of the felt, the cleaning procedure, any surface activation treatment, and the methods of deposition of the gold and lead. Other materials that have been tested as chromium electrodes are carbon and purified-graphite plates.

Approach. - A certain lack of consistency in the physical characteristics of the several batches of carbon felt purchased in 1980 for electrode material has required a unique pretreatment and catalysis procedure for each batch. Much of the in-house effort this year has therefore involved the screening of methods for electrode pretreatment and catalysis in terms of subsequent electrode performance.

Pretreatments have included acid and caustic washes, heating in an oxidizing atmosphere to 800° F and heating in a reducing atmosphere to 1600° F. Distribution of gold catalyst on the chromium electrodes has been accomplished by thermal decomposition following soaking in aqueous and/or organic solvent solutions of gold salts. Another approach has been to electroplate the gold from a gold salt solution. The lead catalyst has been either electroplated after the gold deposition or coplated with the gold.

Evaluation of these electrodes has taken place in complete Redox cells of 14.5- and 320-cm^2 sizes. Generally the cells are repetitively cycled between depth-of-discharge limits of 10 and 90 percent at some nominal current density. These cycles can be normal or accelerated, the latter resulting from turning off the reactant pumps and limiting the capacity to the

quantity of reactant trapped within the cell. Periodically the cell is charged or discharged to 50 percent depth of discharge, and polarization data (voltage vs. current density) are obtained during both charging and discharging.

During normal cycles the variation of open-circuit voltage as a function of state of charge is monitored. The degree of hysteresis between the charge and discharge portions of these data is a measure of the ability of the chromium electrode to catalyze the reaction of, or the equilibrium between, the various Cr^{+3} complexes present. (This is discussed in a following section on fundamental studies.)

The rate of hydrogen evolution from the chromium electrode is monitored by oxidizing the hydrogen electrochemically against $FeCl_3$ in a rebalance cell and measuring the ampere-hours of charge transferred. Cyclic voltammetry has been used as a tool for predicting the catalytic and gassing characteristics of electrodes.

Electrode stability is generally defined in terms of the effect of cycling on performance. An additional test, quite severe, also has been occasionally used. It involves driving the Redox cell negative as much as 1 V and holding it there for an extended period. Subsequent polarization, cycling, and gas evolution data define the electrode stability. Another aspect of electrode stability manifests itself as a dip in the voltage-versus-time curve during a discharge at constant current (fig. 20). This dip is generally assumed to result from an initially incomplete deposition of gold on the carbon (or graphite) felt substrate, followed by lead deposition on both the gold and the bare felt. During discharge the lead deplates from the felt, and subsequent discharge performance reflects the poor catalytic activity of the felt.

Status. - Table 15 presents the pretreatment and catalysis techniques applied to the various carbon and graphite chromium electrode substrates. The KOH-cleaned FMI carbon felt lots 8/79 and 1/80 are compared in figure 21. The variability in the properties of different felt lots is shown by the fact that, although treated identically, the sample from the 1/80 lot did not begin to gas until a higher state of charge and then at a lower rate than the 8/79 sample. A cell containing this better electrode could be charged at 1.3 V, with a hydrogen evolution rate equi- valent to only 0.3 mA/cm^2.

Performance data for a 320-cm^2 cell containing a chromium electrode taken from the 1/80 lot and optimally prepared are presented in figure 22. Initially, when at 50 percent state of charge, this cell could be charged and discharged out to 100 mA/cm^2 with no polarization except that attributable to IR. Only after 16 000 accelerated cycles and several reversals to -1.1 V did the cell develop additional polarizations during charge.

An entirely different type of chromium electrode is represented by the UTC carbon plate in table 15. Carbon plates obtained from United Technologies Corp. were treated to roughen the surface and then prepared as indicated. In cells containing such electrodes the flow of electreolyte is

over the surface of the electrode instead of through the structure as is the case with felt electrodes. In spite of a flow regime that should be much more susceptible to mass transport losses, it can be seen in figure 23 that such polarizations do not develop until a discharge rate of 70 mA/cm^2. Charging was possible out to 90 mA/cm^2 with no losses other than those attributable to IR polarization. These results offer the possibility of completely new cell design concepts, which could also have a favorable effect on system-level considerations such as pump power and shunt current losses.

Lewis Research Center - Fundamental Studies

Background. - Two operational difficulties with chromium Redox solutions are the hysteresis in the open-circuit voltage (fig. 24) and the difficulty of charging a cell in the latter stages of charge. A sizable drop in the charging rate occurs at about 50 to 60 percent state of charge when the cell is being charged at a constant voltage. If the cell is being charged at a constant current density, a substantial increase in voltage is needed at that point to maintain the same current (fig. 25). In addition to reducing the voltage efficiency, this also increases the amount of hydrogen evolution. Changes in color in the chromium solution from blue-green to blue are observed at this point. However, during discharge, the color change from blue back to the original blue-green does not occur at 50 to 60 percent state of charge but at about 85 to 90 percent state of charge. The hysteresis in both the color change and open-circuit voltage and the associated charging difficulties were believed to be due to the two complexed chromic ions predominant in the Redox solutions (fig. 26) and to the slow rates of interconversion between these two ion species.

Approach. - Electrochemical data from the literature are summarized in figure 27. It is obvious that from a thermodynamic standpoint hydrogen will be evolved before chromium is reduced. To have a minimum of hydrogen evolved in the Redox cell, the electrode therefore must have low activity for hydrogen reduction (high hydrogen overvoltage) as well as high activity for chromium reduction. Cyclic voltammetry was used to study electrodes from different felt lots, and prepared in various ways, in terms of chromium activity and hydrogen activity. Acceptance criteria for individual electrodes were also developed.

Since the charging characteristics and the open-circuit voltage hysteresis are associated with the behavior of the different chromium (III) ions, it is necessary to examine what is known about these species. The equilibrium potentials in figure 27(a) show that the hexahydrate will not be reduced until a more negative potential is reached than for the pentahydrate. Figure 27(b) shows that the rate of reduction on mercury electrodes of the pentahydrate species is much more rapid than that of the hexahydrate. Thus the reduction of the pentahydrate is favored not only thermodynamically, but also kinetically.

It can also be calculated from literature data that in Redox solutions at equilibrium at 25° C the relative amounts of the chromium (III) hexahydrate and pentahydrate are about equal but that in chromium (II) solutions about 85 percent of the chromium is present as the pentahydrate and 15

percent as the hexahydrate. Interconversion between chromium (II) species takes place rapidly, but interconversion between chromium (III) species takes place extremely slowly, requiring several months to reach equilibrium.

Provided that the behavior of the gold-lead catalyst is similar to that of mercury electrodes, the sequence of events taking place in charging and discharging Redox cells would be as follows:

(1) The initial blue-green solution consists of roughly equal amounts of the hexahydrate and pentahydrate. When charged, the pentahydrate is reduced more readily. Because of the slow rate of interconversion, it is greatly depleted at 50 to 60 percent state of charge. The remaining blue solution, mostly hexahydrate, requires a higher potential for continued reduction, and this also increases the driving force for hydrogen evolution.

(2) In the charged state the predominant ion is the blue chromium (II) pentahydrate. Since the chromium (III) pentahydrate is produced on discharge, the solution quickly turns back to a blue-green color.

Cyclic voltammetry and spectrophotometry were used to confirm this hypothesis about the behavior of the solutions at gold-lead electrodes and to develop methods for examining the effects of different electrodes on the solution equilibria.

Status of cyclic voltammetry studies of electrodes. - The cyclic voltammetry apparatus is shown schematically in figure 28. Voltage was varied from 0 to -1 V versus an Ag/AgCl reference electrode. Chromium (III) should start being reduced at just past -0.5 V.

Numerous electrodes were examined under various conditions. A sweep rate of 10 mV/s, a chromium concentration of 0.05 M, and an HCl concentration of 2 M were found to be the best conditions for differentiating between chromium activity and hydrogen evolution activity. Figure 29(a), for uncatalyzed felt, shows low activity for both chromium and hydrogen reduction. Figure 29(b) shows a "good" electrode with satisfactory chromium activity (peak current, 45 mA) and sufficiently low hydrogen activity. (Hydrogen current at -1 V is less than the chromium peak current.) A cyclic voltammogram of a poor electrode is also shown (fig. 29(c)). This electrode has sufficient activity for chromium but excessive hydrogen activity, as evidenced by a minimum greater than 15 mA and a hydrogen peak larger than the chromium peak.

These electrode acceptance criteria were selected by comparing cyclic voltammetry scans with measured performance in laboratory-scale cells. Over 200 1/3-ft^2 electrodes were individually screened for the 1-kW preprototype system. These criteria have proved quite satisfactory for this application.

Status of cyclic voltammetry and spectrophotometric studies of chromium complexes. - Cyclic voltammetry sweeps have been carried out on solutions containing predominantly $Cr(H_2O)_6^{+3}$ ions prepared from $Cr(ClO_4)_3$. These data show lesser chromium activity and greater hydrogen evolution with this species, as compared with $[Cr(H_2O)_5Cl]^{+2}$, which is consistent with the electrochemical behavior on mercury and with the proposed equilibrium model.

The published spectra of various chromium species are shown in figure 30. Spectra of the chromium Redox solutions were measured during several charge and discharge cycles by placing the flow cell of the spectrophotometer in line with the chromium reservoir. These spectra were analyzed by using a curve resolver to determine the amounts of hexahydrate and pentahydrate. Three examples of the curves are shown in figure 31. In figure 31(a) the spectrum of a solution during charge is shown at 71 percent state of charge. No pentahydrate is present at this point, having been depleted at about 55 percent state of charge. Figure 31(b) shows the spectrum at 88 percent state of charge, where the charging was terminated. Figure 31(c) shows the spectrum during discharge, at 70 percent state of charge. Comparison with figure 31(a) at the same state of charge shows that the peaks are higher and shifted toward longer wavelengths as a result of the pentahydrate being produced in the discharge reaction, rather than the hexahydrate.

These data prove, as expected, that the observed color changes and voltage changes are indeed due to the chromium (III) pentahydrate being depleted first on charging the cell and being produced first on discharge. The observed composition changes are summarized in figure 32.

Summary. - Cyclic voltammetry has been used successfully to develop acceptance criteria for chromium electrodes. Over 200 electrodes have been tested. Results in laboratory cells and full-size single cells and stacks are in accord with the cyclic voltammetry results.

Spectrophotometric and cyclic voltammetry studies have confirmed the expectations that the cause of slow charging behavior and open-circuit voltage hysteresis is the depletion of $[Cr(H_2O)_5Cl]^{+2}$, leaving $[Cr(H_2O)_6]^{+3}$, which is reduced more slowly and accompanied by greater hydrogen evolution.

For the system to be charged at a more rapid rate, either a better catalyst for the reduction of the hexahydrate or a catalyst for the more rapid equilibration of the hexahydrate and pentahydrate must be found. Work will be carried out in this direction during the coming year.

Figure 33 displays the major milestones associated with this activity.

Single-Cell and Stack Performance

Background

Continuous flow of the reactant solutions is one of the inherent features of the NASA Redox energy storage system. Associated with this continuous flow are pressure drop losses, both in the cells composing the Redox stack and in the associated plumbing between the stack and storage tanks. Pumping requirements are a direct parasitic energy loss to the Redox system since continuous flow is necessary throughout the charge and discharge portions of a cycle. The larger the pressure drop in a specific system, the larger the pumping requirements. Another characteristic, shunt currents, also represents a parasitic energy loss to the system. Shunt currents are caused by electrolytic paths in the fluid between cells at different potentials in a Redox stack. They are manifested as a self-discharge mechanism

that reduces system efficiency. When designing a particular system, one goal is to minimize the sum of the pumping and shunt-current parasitic energy losses. Both of these loss mechanisms are directly influenced by the single-cell design - specifically, the dimensions of the flow slots through which the reactant fluids enter and leave the cell's active area.

Approach

The design of a Redox cell for a particular application requires a combination of experimental data and computations. Cell performance is measured as a function of flow rate, current, and state of charge to arrive at the minimum multiple of the ideal stoichiometric flow rate that will support performance. The design flow rate then can be either a constant value set by the extremes in operating current and state of charge, or it can be varied continuously throughout each cycle to maintain the flow at the minimum acceptable multiple of the instantaneous stoichiometric flow.

Next, for either a fixed flow rate or a range of flow rates, the cell pressure drop is measured for various cell geometries to arrive at specific pumping power requirements for cells and stacks of cells. Shunt losses are calculated for the same cell geometries and various stack sizes and are then added directly to the pumping power requirements. The minimum algebraic sum for a specific stack size corresponds to the most desirable cell geometry.

Status

The current, total solution concentration, and system state of charge combine to determine the stoichiometric flow requirements of a particular system. Figure 34 shows the stoichiometric requirements of a 1000-cm^2 single cell for two different current values. Figure 35 is termed a "flow map" and is used to find the minimum multiple of stoichiometric flow that sustains adequate cell performance. This plot shows the actual performance of a cell during discharge at four current values. Also shown are horizontal lines depicting the IR voltage loss correction for each current and a series of dashed lines that depict the Nernstian "droop" correction accounting for the concentration change of the reactant species across the cell from inlet to outlet. The actual data show an abrupt voltage drop at each current for flow rates just below 1.5 times the stoichiometric requirement. This is therefore the minimum stoichiometric flow multiple acceptable for adequate cell and stack performance during both the charge and discharge portions of a cycle. Figure 36 plots this design flow rate for various currents and system states of charge.

Pressure drop data for three flow port widths are shown in figures 37 to 39. Each figure includes two flow port (and electrode cavity) depths for cells with and without electrodes. Figure 40 groups together the pressure drop data for cells without electrodes; figure 41, the data for cells with electrodes. The pressure drop due to the presence of the electrode was generally about 50 percent of the total for the cell. These pressure drop and flow rate values for the various cell geometries can be used to calculate specific ideal pumping power values, as shown in table 16. Each cell geometry also determines a manifold-to-manifold ohmic resistance, which, when substituted into a NASA shunt-current model, predicts the shunt loss

for several different stack sizes, shown in table 17 and figure 42. Since the goal in stack design is to choose cell dimensions such that the sum of pumping and shunt-current parasitic energy losses is minimized, the optimum cell geometry must be determined. Figure 43 depicts graphically the sum of losses for three stack sizes as a function of cell geometry (resistance), showing a minimum in each case. For the particular cases studied, there exists a broad design range of cell dimensions that minimizes the sum of these parasitic losses.

Figure 44 displays the major milestones associated with this activity.

APPENDIX - TECHNICAL ACTIVITY SUMMARIES

Project element . . . . . 2.0 - Prototype Systems Development

Contractor . . . . . NASA Lewis Research Center
Redox Project Office
21000 Brookpark Rd.
Cleveland, Ohio 44135

Title . . . . . 1-kW Preprototype Systems Test

Principal investigator . . . . . Norman H. Hagedorn

Contract number DE-AI04-80AL12726

Period of performance . . . . . Calendar year 1980

Work location . . . . . Cleveland, Ohio

Contracting office . . . . . NASA Lewis Research Center

Cumulative funding (reimbursable only) $88 700

Background: Redox cell component technology has reached a level that makes feasible the assembly and test of a complete system.

Objectives: To evaluate the general design approach taken, to examine interactions at the Redox-photovoltaic interface, to study loss mechanisms, and to measure performance characteristics of complete systems.

Approach: Assemble a 1-kW/10-kWh Redox system and operate in conjunction with a 5-kW (peak) solar photovoltaic array. Under various load conditions, measure system performance, losses, effective capacity, etc.

Output: Operating experience; design data based on actual system performance; system efficiencies; report.

Project element . . . . . 3.0 - Application Analyses

Contractor . . . . . Earl Warren Legal Institute
Energy Studies Project
2941 Telegraph Ave., Suite B
Berkeley, California 94705

Title . . . . . First-phase Research and Conceptual Analysis for Commercialization of Redox Energy Storage and Phosphoric Acid Fuel Systems

Principal investigator . . . . . John Nimmons

Contract number NAG3-11

Period of performance . . . . . 10/1/80 to 6/30/81

Work location . . . . . Berkeley, Calif.

Contracting office. . . . . NASA Lewis Research Center

Cumulative funding (through fiscal year 1980; reimbursable only) 0

Background: The grant is partially funded by the Redox Project Office. Early study emphasis is on fuel cell issues.

Objective: To identify institutional issues related to Redox system deployment and technology transfer.

Approach: Evaluation of decontrol, fuel use, and the Public Utilities Regulatory Policy Act and other pertinent legislation for their influence on commercial uses of Redox.

Output: Final report due by July 1981. Preliminary results indicate that some existing legislation may provide some stimulus to the introduction of Redox to users.

Project element . . . . . 3.0 - Application Analyses

Contractor . . . . . United Technologies Corporation
Power Systems Division
P. O. Box 109
South Windsor, Conn. 06074

Title . . . . . Cost Projections for Redox Energy Storage Systems

Principal investigator . . . . . J. Stedman

Contract number DEN3-126

Period of performance . . . . . 4/30/79 to 3/31/81

Work location . . . . . South Windsor, Conn.

Contracting office. . . . . NASA Lewis Research Center

Cumulative funding (through fiscal year 1980; reimbursable only). . $52 699

Background: Cost projections are required to establish the economic viability of Redox systems. No such cost estimates are currently available.

Objectives: To establish Redox storage system conceptual production designs, to estimate production cost, and to determine the influence of various parameters on production cost.

Approach: Estimate manufacturer's selling price for 10-kW/500-kWh Redox systems at an annual production rate of 1000 units. Estimate manufacturer's selling price for 10-MW/100-MWh Redox systems at an annual production rate of 100 units.

Output: Final report to be published in March 1981. Results show Redox systems to be amenable to mass production techniques. Major cost elements are reactants and tankage. System costs are very competitive with other storage systems.

Project element	3.0 - Application Analyses
Contractor	Aerospace Corporation P. O. Box 92957 Los Angeles, Calif. 90009
Title	Redox Assessments and Computer Model Studies
Principal investigator	H. E. Carmichael
Contract number	NASA-Air Force Interagency Order C-42701-D
Period of performance	Calendar years 1980 and 1981
Work location	Los Angeles, California
Contracting office	NASA Lewis Research Center
Cumulative funding (through fiscal year 1980; reimbursable only)	$150 000

Background: Computer model availability greatly increases ability to examine application concepts over a range of inputs. Assessment of market penetration provides direction to appropriate application and system sizes for development.

Objectives: To assess the market penetration potential for residential and other Redox applications. To define, design, and implement a computer model of the Redox system using Lewis data for system characteristics.

Approach: Lewis will define the scope and intended uses of the computer model, its input and output parameters, and the computer systems environment in which the model will be installed and operated. Aerospace will write the computer program and install it on the Lewis computer. Actual percentage market penetration each year will be determined by the estimated number of potential purchasers for whom a financial figure of merit exceeds a threshold value for the adoption decision.

Output: Final report of market penetration potential due by May 1981. Fully documented computer model installed on a Lewis computer and ready for operation.

Project element . . . . . 4.0 – Supporting Technology

Contractor. . . . . NASA Lewis Research Center
Redox Project Office
21000 Brookpark Rd.
Cleveland, Ohio 44135

Title . . . . . In-House Membrane Development and Evaluation

Principal investigator . . . . . Jerri S. Ling

Contract number DE-AI04-80AL12726

Period of performance . . . . . Calendar year 1978 to present

Work location . . . . . Cleveland, Ohio

Contracting office. . . . . NASA Lewis Research Center

Cumulative funding (through fiscal year 1980; reimbursable only) $445 800

Background: Contractual effort is endeavoring to develop membranes combining good selectivity, resistivity, and cost characteristics. Those membrane candidates that pass screening criteria at the developers are sent to Lewis for further screening and in-cell evaluations.

Objectives: Perform laboratory tests to determine membrane area resistivity and selectivity. These tests approximate conditions a membrane is likely to encounter in a Redox environment.

Output: Direction for further membrane development by contractor.

Project element . . . . . 4.0 - Supporting Technology

Contractor. . . . . Ionics, Inc.
64 Grove Street
Watertown, Mass. 02172

Title . . . . . Development and Preparation of Redox Cell Anion Exchange Membranes

Principal investigator. . . . . Russell B. Hodgdon

Contract number DEN3-204

Period of performance . . . . . 11/12/80 to 11/11/81

Work location . . . . . Watertown, Mass.

Contracting office. . . . . NASA Lewis Research Center

Cumulative funding (through fiscal year 1980; reimbursable only) $306 600

Background: Membrane properties need to be improved in order to make multimegawatt Redox systems feasible. Great advances have already been made since the membrane development program began in 1975. DEN3-204 work began in December 1980.

Objectives: To produce, for the NASA Redox energy storage system, anion exchange membranes that meet goals of 1.5-Ω-cm^2 area resistivity and 5-μg Fe/h/cm^2/M/liter selectivity. To provide a supply of scaled-up membranes in large quantities.

Approach: Vary properties of membranes by changing basic parameters of membrane chemistry, polymerization catalyst, fabric back thickness, ion conductivity, and pore size.

Output: Final report to be published in January 1982. Preliminary development of new thinner fabric backings resulted in lowered area resistivity in 1 M Fe. Cell output with this membrane is 49 A/ft^2 at 0.9 V at 50 percent depth of discharge.

Project element . . . . . 4.0 - Supporting Technology

Contractor. . . . . NASA Lewis Research Center
Redox Project Office
21000 Brookpark Rd.
Cleveland, Ohio 44135

Title . . . . . In-House Electrode Development and Evaluation

Principal investigator . . . . . Randall F. Gahn

Contract number DE-AI04-80AL12726

Period of performance . . . . . Calendar year 1978 to present

Work location . . . . . Cleveland, Ohio

Contracting office . . . . . NASA Lewis Research Center

Cumulative funding (through fiscal year 1980; reimbursable only) $281 600

Background: Stable, reversible electrodes are required for the Redox energy storage system. Anticipated system lifetimes of 20 years would require electrodes to undergo more than 7000 cycles operating on a one-cycle-per day basis. Single-cell systems have exceeded 20 000 cycles without significant performance changes. Uncatalyzed carbon felt is used for the iron electrode, and gold-lead catalyzed carbon felt for the chromium electrode. Considerable variations in performance of the chromium electrode are caused by variation in the carbon felt.

Objectives: To consistently prepare chromium electrodes with acceptable electrochemical performance, to evaluate contractor-prepared electrodes, and to begin work on planar, catalyzed electrodes.

Approach: Evaluate electrodes in cell hardware and by cyclic voltammetry. Measure performance as a function of carbon felt lot, cleaning treatment, and catalysis procedure. Use specific tests for hydrogen evolution, coulombic efficiency, catalyst stability, and electrochemical activity.

Output: A "standard" method for fabricating, cleaning, and catalyzing carbon felt for use as chromium electrodes. A report covering chromium electrode testing will be published in mid-1981. Routine experimental techniques for evaluating electrodes.

Project element . . . . . 4.0 - Supporting Technology

Contractor . . . . . Giner, Inc.
14 Spring St.
Waltham, Mass. 02154

Title . . . . . Optimization and Fabrication of Porous Carbon Electrodes for Iron-Chromium Redox Flow Cells

Principal investigator . . . . . .Vinod M. Jalan

Contract number DEN3-198

Period of performance . . . . . 6/11/80 to 6/10/81

Work location . . . . . Waltham, Mass.

Contracting office . . . . . NASA Lewis Research Center

Cumulative funding (through fiscal year 1980; reimbursable only) $192 800

Background: Since 1976, Giner, Inc., has investigated various Redox couples, electrocatalysts, substrate materials, and catalyst application procedures. The gold-lead catalyst was discovered to give good electrochemical activity for the chromium electrode. Large differences in the physical and chemical properties of carbon felts were determined to be a major cause of electrode performance variations. An alcohol-gold catalysis procedure was discovered that leads to improved electrode performance.

Objectives: To characterize the carbon/graphite electrode substrate material, to evaluate gold-lead catalysis methods, to prepare assembly-ready electrodes up to 1 ft^2, and to evaluate alternative electrocatalysts.

Approach: Study several commercially available carbon-graphite felts by cyclic voltammetry for hydrogen evolution, chromium oxidation and reduction, and lead oxidation and reduction. Evaluate samples of felts prepared at six temperatures. Examine alternative electrocatalysts for activity.

Output: Specifications for a "Redox grade" carbon felt. Identification of "standard" cleaning and catalysis procedures for preparation of chromium electrodes. Chromium electrodes up to 1 ft^2 for testing. Final report for the contract by November 1981.

Project element . . . . . 4.0 - Supporting Technology

Contractor . . . . . Spring Arbor College
Spring Arbor, Mich. 49283

Title . . . . . Chemical and Electrochemical Aspects of Chromic/Chromous Electrode Reaction in NASA Redox Energy Storage System

Principal investigator . . . . . David A. Johnson

Contract number NAG3-148

Period of performance . . . . . 1/81 to 12/81

Work location . . . . . Spring Arbor, Mich.

Contracting office . . . . . NASA Lewis Research Center

Cumulative funding (through fiscal year 1980; reimbursable only) $12 000

Background: There have been no detailed analyses at NASA Lewis of the complex ion chemistry of the chromium solution, which is one of the fully soluble Redox couples (Cr^{+2}/Cr^{+3}) currently in use. In-house studies have shown several hysteresis effects (lower open-circuit voltage on discharge than charge and different color changes on charge and discharge) in the Redox flow cell system. The effects are believed to be due to a slow establishment of equilibrium between several complex Cr^{+3} species.

Objectives: To more clearly identify the chromium species in the chromium solution of the NASA Redox energy storage system as well as to determine the mechanism of the reduction and oxidation at the catalyzed carbon felt electrode.

Approach: Prepare and study spectroscopically a series of pure isomers with varying concentrations to find a good catalyst to promote rapid equilibration of these species. Follow the electrochemical reaction at the chromium electrode of a Redox flow cell and study it in terms of complex ion equilibria.

Output: Final report by January 1982. These studies should lead to improved charge rates and energy efficiencies for the iron-chromium Redox system.

Project element . . . . . 4.0 - Supporting Technology

Contractor. . . . . NASA Lewis Research Center
Redox Project Office
21000 Brookpark Rd.
Cleveland, Ohio 44135

Title . . . . . Single-Cell and Stack Performance Tests

Principal investigator. . . . . Norman H. Hagedorn

Contract number DE-AI04-80AL12726

Period of performance . . . . . 1981 to present

Work location . . . . . Cleveland, Ohio

Contracting office. . . . . NASA Lewis Research Center

Cumulative funding (through fiscal year 1980; reimbursable only) $383 000

Background: As improvements in cell components are achieved, they are incorporated into scaled-up cells and then into stacks. Also, various design approaches are evaluated this way.

Objectives: To implement the scaleup process from small cells to stacks of large cells, to give direction to further development efforts, and to identify characteristics that will affect system design.

Approach: Design, assemble, and test cells and stacks of 0.33-ft^2 and 1.0-ft^2 cells.

Output: Design improvements, feedback for guiding further cell component development, and identification of parameters sensitive to scaleup and parameters affecting system design.

REFERENCES

1. Hodgdon, R. B.; and Waite, W. A.: Anion Permselective Membrane. DOE/NASA/0137-1, NASA CR-165223, 1980.

2. Alexander, S. S.; Hodgdon, R. B.; and Waite, W. A.: Anion Permselective Membrane. DOG/NASA/0001-79/1, NASA CR-159599, 1979.

3. Alexander, S. S.; and Hodgdon, R. B.: Anion Permselective Membrane. NASA CR-135316, 1977.

4. Alexander, S. S.; Geoffroy, R. R.; and Hodgdon, R. B.: Anion Selective Membrane. NASA CR-134931, 1975.

5. Ling, J. S.; and Charleston, J.: Advances in Membrane Technology for the NASA Redox Energy Storage System. DOE/NASA/12726-12, NASA TM-82701, 1980.

6. O'Donnell, P.M.; Sheibley, D. W.; and Gahn, R.F.: Anion Exchange Membranes for Electrochemical Oxidation-Reduction Energy Storage System. ERDA/NASA-1002/77/2, NASA TM-73751, 1977.

7. Hanley, H. J. M., ed.: Transport Phenomena in Fluids. M. Dekker, 1969.

8. Holleck, G. L.; et al.: Silver-Hydrogen Energy Storage. AFAPL-TR-78-65, EIC, Inc., 1978. (AD-A061426.)

9. Schlögl, R.: Membrane Permeation in Systems Far From Equilibrium. Ber. Bunsenges. Phys. Chem., 1966, pp. 400-406.

BIBLIOGRAPHY

Gahn, R. F.; et al.: Performance of Advanced Chromium Electrodes for the NASA Redox Energy Storage System. DOE/NASA/12726-15, NASA TM-82724, 1981.

Hagedorn, N. H.; and Thaller, L. H.: Redox Storage Systems for Solar Applications. DOE/NASA/1002-80/5, NASA TM-81464, 1980.

Ling, J. S.; and Charleston, J. A.: Advances in Membrane Technology for the NASA Redox Energy Storage System. DOE/NASA/12726-12, NASA TM-82701, 1980.

Prokopius, P. R.: Model for Calculating Electrolytic Shunt Path Losses in Large Electrochemical Energy Conversion Systems. NASA TM X-3359, 1976.

Reid, M. A.; et al.: Preparation and Characterization of Electrodes for the NASA Redox Storage System. Presented at the Electrochemical Society Meeting, (Hollywood, Fla.), Sept. 5-10, 1980.

Reid, M. A.; and Thaller, L. H.: Improvement and Scale-up of the NASA Redox Storage System. DOE/NASA/12726-6, NASA TM-81632, 1980.

Stedman, J. K.; Michaels, K. B.; and Hall, E. W.: Cost Projections for Redox Energy Storage Systems. DOE/NASA/0126-1, NASA CR-165260, 1980.

TABLE 1. - NOMINAL DESIGN SPECIFICATIONS FOR NASA LEWIS PREPROTOTYPE 1-kW REDOX STORAGE SYSTEM

Gross power, W	1260
Nominal net power, W	1000
Voltage, V dc	120 ± 5%
Number of stacks	4
Number of cells per stack	39
Number of trim packages (6 cells each)	10
Depth-of-discharge range (utilization)	80% - 20% (0.60)
Reactant volume (each), liters (U.S. gallons)	700 (186)
Reactant energy density (end of life), Wh/liter	14.5
Cell active area, cm^2	320
Nominal current density, mA/cm^2	30
Reactants	1 M/1 $FeCl_3$, 2 N HCl
	1 M/1 $CrCl_2$, 2 N HCl
Reactant flow rates (nominal), cm^2/min cell	100-150
Parasitic losses, W:	
Pumps	120 (15% efficiency)
Shunt power	120
Number of rebalance cells	5
Number of charge-indicator cells	1

TABLE 2. - REDUCTION OF SHUNT-CURRENT LOSS (TAPER CURRENT) BY CELL DESIGN CHANGES: FIVE-CELL STACKS, 1.20 V/CELL

Configuration	Taper current, mA
Original	2000
Bipolar-plate manifold holes insulated from fluids	140
Membrane manifold holes insulated from fluids	28
Membranes insulated from fluids in port slots	12
Mathematical model	7

TABLE 3. - PARASITIC LOSSES FOR PREPROTOTYPE 1-kW REDOX STORAGE SYSTEM

	Measured	Design estimate
	Loss, W	
Pumps	120 (max.)	120
Shunt currents	230 (max.)	120
Instruments and controls	100	---

TABLE 4. - PERFORMANCE DATA FOR COMBINED REDOX-PHOTOVOLTAIC SYSTEM (CONFIGURATION 1)

Insolation, mW/cm^2	78.2
Number of trim cells active	12
Array voltage, V	115.5
Array current, A	29.1
Load voltage, V	120.5
Load current, A	18.6
Main stack voltage, V	111.5
Main stack current, A	10.5
Trim cell voltage (charge), V	9.0
Trim cell current (discharge), A	18.6
Discharge power (trim cells), W	167
Array power, W	3245
Load power, W	2241
Charge power, W	1171
State of charge, percent	33

TABLE 5. - MANUFACTURER'S SELLING PRICE - 10-kW/500-kWh SYSTEM

Cell stack, $/kW	367.56
BOS[a], tanks, and chemicals ($CrCl_3 \cdot 6 H_2O$ at $0.32/lb), $ kWh	68.03
Cell stack, $/kW	363.10
BOS[a], tanks, and chemicals ($CrCl_3 \cdot 6 H_2O$ at $1.30/lb, $/kWh	109.91

[a]Balance of system.

TABLE 6. - MANUFACTURER'S SELLING PRICE - 10-MW/100-MWh SYSTEM

Cell stack, $/kW	.13b.59
BOS[a], tanks, and chemicals ($CrCl_3 \cdot 6 H_2O$ at $0.32/lb), $/kWh	54.45
Cell stack, $/kW	.134.24
BOS[a], tanks, and chemicals ($CrCl_3 \cdot 6 H_2O$ at $1.30/lb), $/kWh	99.60

[a]Balance of system.

TABLE 7. - REDOX RESIDENTIAL APPLICATION

FOB cost of factory (1980 dollars), dollars	4425
Annual inflation rate, percent	8
Wholesale markup (new construction), percent	20
Retail markup (new construction), percent	33-1/3
Installation cost and ancillary equipment (1980 dollars), dollars	1000
Annual operating and maintenance cost, percent of installed cost	2
Nominal capacity, kW/kWh	5.25
Energy retrieval efficiency, percent	75
Lifetime, yr	30

TABLE 8. - PRELIMINARY 30-YEAR-LIFE-CYCLE COSTS[a]

	Peak/ off peak ratio	Redox	Advanced lead acid[b]	No storage (grid only)
	Cost, dollars			
New construction[c] (all-electric, energy-efficient home)	2	142 309	152 123	131 260
	3	132 061	142 263	131 691
Retrofit[d] (all-electric, conventional home)	2	180 470	179 952	159 202
	3	167 934	167 804	157 346

[a]Present value in 1985 dollars over 30-yr life.
[b]Five-year battery replacement cycle at $62/kWh.
[c]Storage system costs included in 30-yr mortgage.
[d]Storage system costs financed over 5-yr period.

TABLE 9. - MEMBRANE CHARACTERIZATION DATA FOR VINYLBENZYLCHLORIDE (VBC) VARIATIONS

Characteristic	Excess VBC[a], percent			Standard
	5	10	20	
Water content, percent	36.5	36.4	34.7	35.8
NP content, percent	0.25	0.25	0.25	0.25
Area resistivity (in 0.1 N HCl), Ω-cm^2	4.2	4.6	4.9	4.4
Thickness, cm	0.043	0.042	0.044	0.042
Ion-exchange capacity, meq/dry g:				
Total	4.17	4.06	4.00	4.33
Strong	2.30	2.10	2.17	2.11
Weak	1.87	1.96	1.83	2.22

[a]Extra mole % of VBC over standard formulation.

TABLE 10. - IRON FOULING AND PERMEABILITY DATA
FOR VINYLBENZYLCHLORIDE (VBC) VARIATIONS

Characteristic	Excess VBC, percent			Standard
	5	10	20	
Area resistivity (in 0.1 N HCl), Ω-cm^2	4.2	4.6	4.9	4.4
Area resistivity (2 M $FeCl_3$, 2 N HCl after 360 h), Ω-cm^2	16.3	14.4	22.4	---
Permeability, μg Fe/h/cm^2/moles/liter	15	16	9	14

TABLE 11. - MEMBRANE CHARACTERIZATION DATA
FOR CATALYST CONCENTRATION VARIATIONS

Characteristics		Catalyst, percent			
		0	0.0625	0.25	0.50	1.00
Water content, percent		65-75	36.2	36.4	35.8	35.7
NP content, percent		0.25	0.25	0.25	0.25	0.25
Area resistivity (in 0.1 N HCl), Ω-cm^2		---	4.3	4.5	4.6	4.6
Thickness, cm		---	0.043	0.043	0.044	0.044
Ion-exchange capacity (meq/dry g):						
Total	Undercured		4.25	4.26	4.33	3.94
Strong	rubbery and		2.00	2.09	2.11	1.94
Weak	flexible		2.25	2.17	2.22	2.00

TABLE 12. - RESULTS OF RESISTIVITY FLOW TESTS ON VARIOUS MEMBRANE FORMULATIONS

Variation	Area resistivity, Ω-cm^2								Selectivity, μg Fe/h/cm^2/M/ liters 1.0 M Fe/0.5 N HCl
	1.0 N HCl	2.0 N HCl	0.5 M Fe^{+3} 1 N HCl	0.5 M Fe^{+3} 2 N HCl	1 M Fe^{+3} 1 N HCl	1 M Fe^{+3} 2 N HCl	1.5 M Fe^{+3} 1 N HCl	1.5M Fe^{+3} 2 N HCl	
CDIL-A5[a]-0.5 catalyst-25NP[6]	3.92	---	3.92	---	6.82	---	21.75	---	15
CDIL-AA5[c]-0.0625 catalyst-25NP	3.5	2.3	3.9	2.6	5.2	5.4	10.3	19.7	20
CDIL-AA5[c]-0.0625 catalyst-27.5NP	3.6	2.0	3.9	2.8	5.4	5.4	10.3	18.4	21
NP content variation									
CDIL-A5[a]-0.5 catalyst-20NP	4.79	---	4.79	---	8.56	---	34.80	---	7
Catalyst variation									
CDIL-AA5-0.25 catalyst-27.5NP	3.5	2.8	---	3.0	---	6.2	20.0	---	16
Crosslink variation									
(VBC)[d]V + 10 - 0.5 catalyst-25NP	3.6	2.8	---	3.0	---	6.5	22.5	---	16
(DMAEMA)[e]D + 20 - 0.5 catalyst-25NP	3.3	2.8	---	2.8	---	5.8	16.7	---	30
$(TMPTMA)^+$ + (DMAEMA)	6.4	3.8	6.7	4.8	8.6	7.5	13.5	17.0	17
50 Percent CDIL + 50 percent CP4 L	3.6	3.0	---	3.9	---	10.6	44.5	---	12
50 Percent 1,6 HDMA[g] + 50 percent VBC	3.8	2.2	4.2	3.0	6.1	5.7	12.2	22.0	27
25 Percent 1,6 HDMA + 75 percent VBC	4.1	2.3	4.5	3.0	6.8	5.9	12.9	23.2	25
100 Percent 1,6 HDMA	3.9	2.2	4.1	3.0	6.5	6.1	13.2	27.1	30
Functionality variation									
Long defunctional	2.18	---	---	---	3.19	---	4.35	---	179
Short defunctional	2.76	---	---	---	3.77	---	4.93	---	75
Trifunctional	2.76	---	---	---	3.77	---	4.93	---	81
Tetrafunctional, 100 percent	2.76	---	2.90	---	4.64	---	8.12	---	66
Ti/tri/tetrafunctional (Mix)	2.76	---	3.92	---	5.80	---	14.94	---	37
Di/tetrafunctional (50 percent tetra + 50 percent di)	2.47	---	2.61	---	3.77	---	6.96	---	81
Thin fabric B	2.76	---	2.90	---	4.35	---	14.21	---	28
Thin fabric C	2.61	---	2.61	---	3.92	---	13.78	---	30

[a] Past standard.
[b] Nonpolymerizable content.
[c] New standard.
[d] Vinylbenzylchloride.
[e] Dimethylaminoethylmelhacrylate.
[f] Trimethylolpropane-trimelhacrylate.
[g] 1,6 Hexamediol-dimethacrylate.

TABLE 13. – CALCULATED EFFECT OF TRANSFERENCE NUMBERS ON OSMOTIC PRESSURE AND H^+ CONCENTRATION DIFFERENCES (WATER TRANSPORT TOWARD CHROMIUM ELECTRODE)

Transference number, milliliter/f	Number of cycles	End of–	Solution volume, cm^3		Ionic concentration gradient across membrane, $\Delta\Sigma C_j$, g ion/liter	Hydrogen concentration gradient across membrane, ΔH^+, g ion/liter
			Fe	Cr		
$t_{H^+} = 0.8$	1	[a]C	867	1133	76×10^{-2}	1.4
		[b]D	997	1003	97	~0
$t_{Cl^-} = 0.2$	5	C	857	1143	63	1.34
		D	987	1013	85	-.02
$t_{H_2O} = 130$	10	C	844	1156	50	1.32
		D	974	1026	72	-.03
	20	C	792	1208	-10	1.24
		D	922	1078	15	-.15
	45	C	753	1246	-55	1.44
		D	883	1117	-29	-.28
$t_{H^+} = 0.6$	1	C	867	1133	-6	.14
		D	997	1003	97	~0
$t_{Cl^-} = 0.4$	5	C	857	1143	-18	.12
		D	987	1013	85	-.02
$t_{H_2O} = 130$	10	C	844	1156	-33	.09
		D	974	1026	72	-.03
$t_{H^+} = 0.2$	1	C	867	1133	-169	.14
		D	997	1003	97	~0
$t_{Cl^-} = 0.8$	5	C	857	1143	-181	.12
		D	987	1013	85	-.02
$t_{H_2O} = 130$	10	C	844	1156	-197	.09
		D	974	1026	72	-.03
$t_{H^+} = 0.8$	1	C	918	1082	131	1.45
		D	998	1002	98	~0
$t_{Cl^-} = 0.2$	5	C	912	1088	125	1.03
		D	992	1008	91	~0
$t_{H_2O} = 80$	10	C	904	1096	115	1.42
		D	984	1015	83	-.04
	20	C	888	1112	99	1.42
		D	968	1032	64	-.06
$t_{H^+} = 0.6$	1	C	918	1082	50	1.03
		D	998	1002	98	~0
$t_{Cl^-} = 0.4$	5	C	912	1088	44	1.03
		D	992	1008	91	~0
$t_{H_2O} = 80$	10	C	904	1096	35	1.02
		D	984	1015	83	-.04
	20	C	888	1112	17	.98
		D	968	1032	64	-.07
$t_{H^+} = 0.2$	1	C	918	1082	-111	.24
		D	998	1002	98	~0
$t_{Cl^-} = 0.8$	5	C	912	1088	-118	.22
		D	992	1008	91	~0
$t_{H_2O} = 80$	10	C	904	1096	-126	.21
		D	984	1015	83	-.04
	30	C	872	1128	-163	.15
		D	952	1048	48	-.10

[a]Charge.
[b]Discharge.

TABLE 14. - CALCULATED EFFECT OF TRANSFERENCE NUMBERS ON OSMOTIC PRESSURE AND H^+ CONCENTRATION DIFFERENCES (WATER TRANSPORT TOWARD IRON ELECTRODE)

Transference number, milliliter/f	Number of cycles	End of-	Solution volume, cm^3		Ionic concentration gradient across membrane, $\Delta \Sigma C_j$, g ion/liter	Hydrogen concentration gradient across membrane, ΔH^+, g ion/liter
			Fe	Cr		
$t_{H^+} = 0.8$	1	[a]C	867	1133	379×10^{-2}	1.9
		[b]D	997	1003	103	~0
$t_{Cl^-} = 0.2$	5	C	857	1143	385	1.8
		D	987	1013	114	.02
$t_{H_2O} = 130$	10	C	844	1156	401	1.9
		D	974	1026	129	.06
$t_{H^+} = 0.6$	1	C	867	1133	291	1.5
		D	997	1003	103	~0
$t_{Cl^-} = 0.4$	5	C	857	1143	303	1.52
		D	987	1143	303	1.52
$t_{H_2O} = 130$	10	C	844	1156	320	1.55
		D	974	1026	129	.06
$t_{H^+} = 0.2$	1	C	867	1133	129	.67
		D	997	1003	103	~0
$t_{Cl^-} = 0.8$	5	C	857	1143	140	.70
		D	987	1013	114	.02
$t_{H_2O} = 130$	10	C	844	1156	156	.73

[a]Charge.
[b]Discharge.

TABLE 15. – EXPERIMENTAL CHROMIUM ELECTRODES

Substrate and lot	Cleaning treatment	Gold catalysis method	Catalyst solvent	Gold content, $\mu g/cm^2$	Discharge dip?	Comments
FMI carbon felt – 8/79	H_2SO_4	Thermal	H_2O	12.5	No	High H_2
	HNO_3	Thermal		12.5	No	High H_2 after reversal
	HNO_3	Electroplated		12.5	Yes	High H_2
	HF	Electroplated		6	No	Moderate H_2
	KOH	Thermal	$MeOH/H_2O$	12.5	No	Low H_2, best performance
	H_2x(1600° F)	Electroplated	H_2O	25	---	High H_2
	None	Self-plated	H_2O	12.5	---	High H_2
FMI carbon felt – 1/80	HNO_3	Pb only	H_2O	0	Yes	Low H_2
	H_2SO_4	Pb only	H_2O	0	Yes	Moderate H_2
	HCl	Thermal	$ETOH/H_2O$	12.5	No	Moderate H_2, slow Cr^{+3} reduction
	KOH	Thermal	$MeOH/H_2O$	12.5	No	Low H_2, good Cr^{+3} reduction, best performance
	H_2SO_4	Electroplated	H_2O	25	Yes	Moderate H_2
	None	Thermal	H_2O	17	No	High H_2
	HNO_3	Thermal	H_2O	12.5	---	High H_2
FMI carbon felt – 1/80	KOH	Thermal	$MeOH/H_2O$	50	No	Moderate H_2
FMI carbon felt – 8/80	KOH	Thermal	$MeOH/H_2O$	12.5	No	High H_2
FMI carbon felt – 12/80	KOH	Thermal	$MeOH/H_2O$	12.5	No	Moderate H_2
	HCl	Thermal	KOH/H_2O	12.5	No	Low H_2, best performance
Carborundum 0.635-cm (1/4-in.) graphite	KOH	Thermal	$MeOH/H_2O$	12.5	No	Moderate H_2
Ultracarbon purified graphite	None	Pb only	--------	0	Yes	High H_2
	KOH	Thermal	$MeOH/H_2O$	12.5	No	Moderate H_2
FMI carbon felt – 10/80	HNO_3	Thermal	$MeOH/H_2O$	12.5	No	Moderate
UTC carbon plate	None	Thermal	H_2O	1.7	Yes	Moderate H_2, poor discharge characteristics
	KOH			14	No	Low H_2
	HCl			14	No	Low H_2, best performance
	H_2SO_4			14	No	Moderate H_2

TABLE 16. - IDEAL PUMPING POWER PER STACK, BASED ON FLOW STUDIES

Cavity thickness, cm	Flow port dimensions, cm	Approximate resistance (manifold to manifold)	Flow rate per cell to each electrode, cm^3/min								
			150			300			450		
			Number of cells per stack								
			20	40	80	20	40	80	20	40	80
			Ideal pumping power[a], W								
0.125	0.2 x 0.075	7600	5.2	10	21	--	--	--	--	--	--
	.4 x .075	3800	3.0	6.0	12	14	27	55	--	--	--
	.7 x .075	2500	2.5	4.9	9.8	10	21	41	24	48	96
0.250	0.2 x 0.200	2900	1.8	3.6	7.3	8.5	17	34	22	45	90
	.4 x .200	1400	1.3	2.7	5.3	5.4	11	22	12	25	49
	.7 x .200	1000	.96	1.9	3.8	3.8	7.7	15	9.0	18	36

[a]Approximate cell-to-cell resistance, 1.25 Ω; solution viscosity, 1.55 cS.

TABLE 17. - CALCULATED SHUNT-CURRENT POWER LOSSES PER STACK, AS PREDICTED BY NASA MODEL

Manifold resistance (cell to cell), Ω	Cell resistance (manifold to manifold), Ω	Voltage per cell (nominal), V/cell					
		1.0			2.0		
		20	40	80	20	40	80
		Shunt loss, W					
1.0	1 000	4.9	31	140	20	125	560
	2 000	2.5	18	99	10	72	396
	3 000	1.7	12	77	6.9	51	307
	6 000	.87	6.7	46	3.5	27	183
	12 000	.44	3.5	25	1.8	14	101
2.0	1 000	4.5	25	93	18.7	102	372
	2 000	2.5	16	72	9	64	290
	3 000	1.7	12	60	6.7	46	239
	6 000	.87	6.4	40	3.5	26	157
	12 000	.44	3.4	23	1.8	13	93

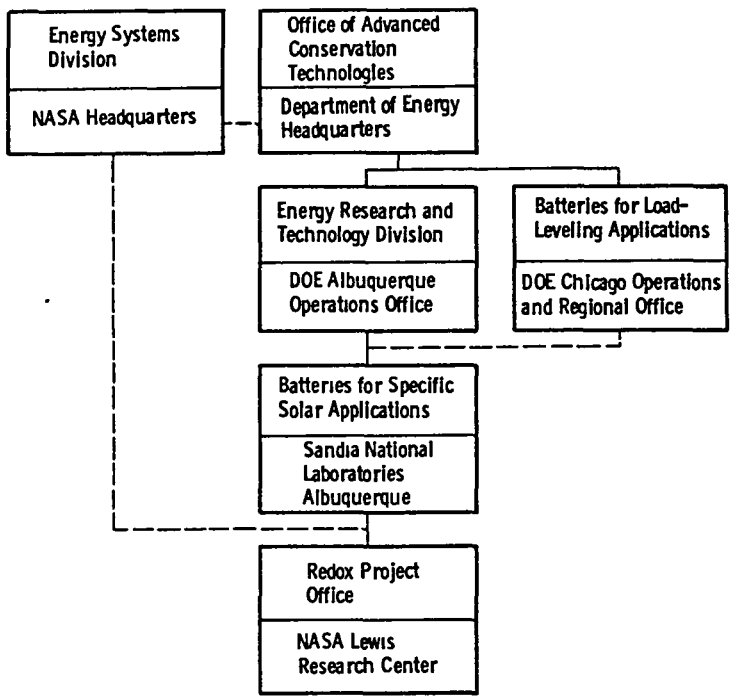

Figure 1. - Redox project management structure - calendar year 1980.

▽ Milestone
□ Request for proposal issued
○ Contract awarded
◇ Department of Energy management decision

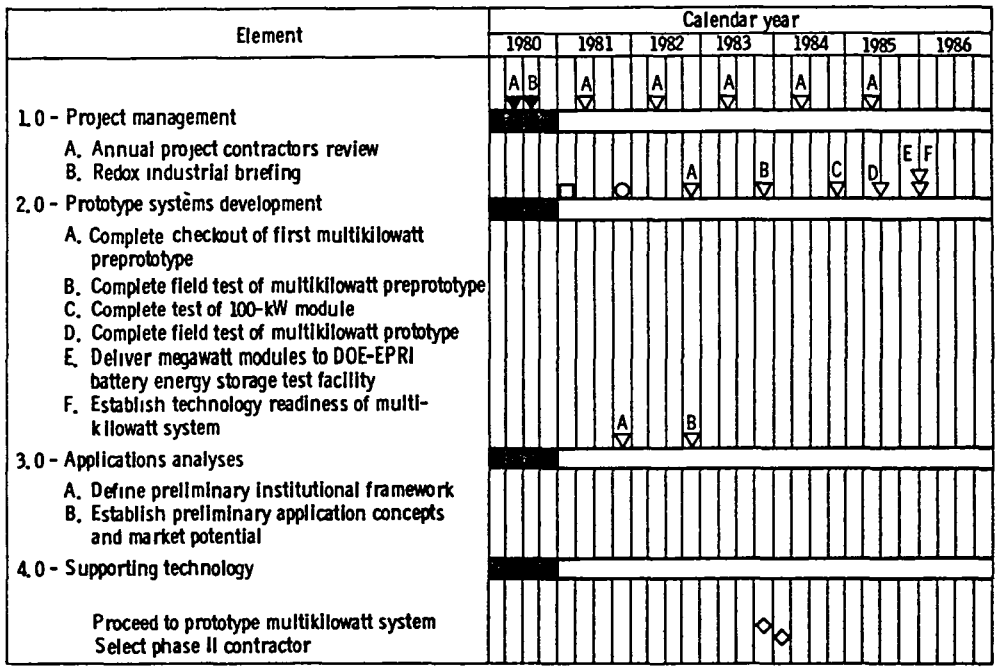

Figure 2 - NASA Redox Storage System Development project.

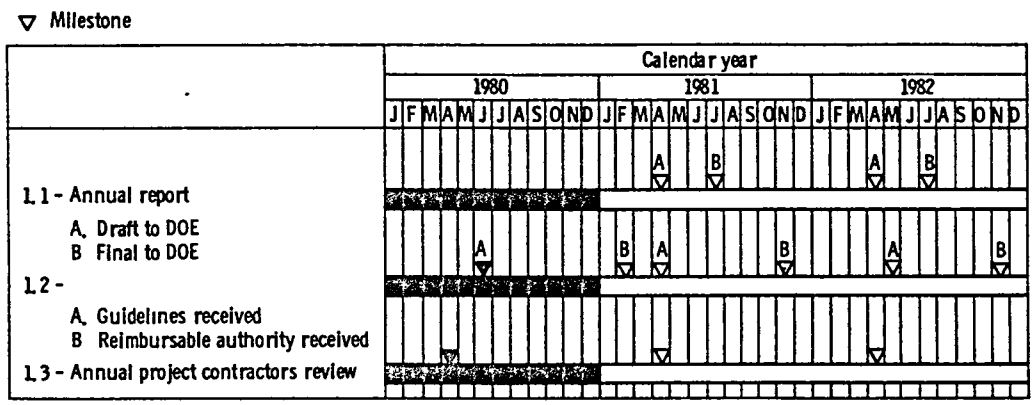

Figure 3. - Activity schedule for Redox project element 1.0 - project management.

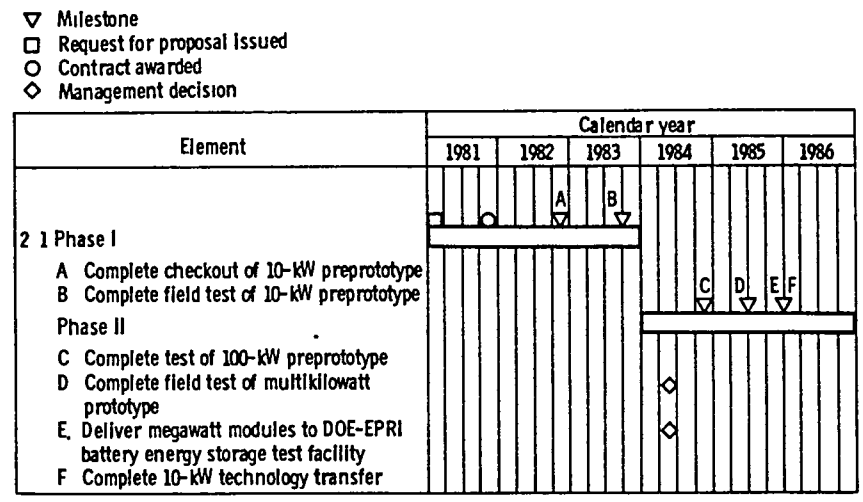

Figure 4. - Contract activity for Redox project element 2.0 - prototype systems development.

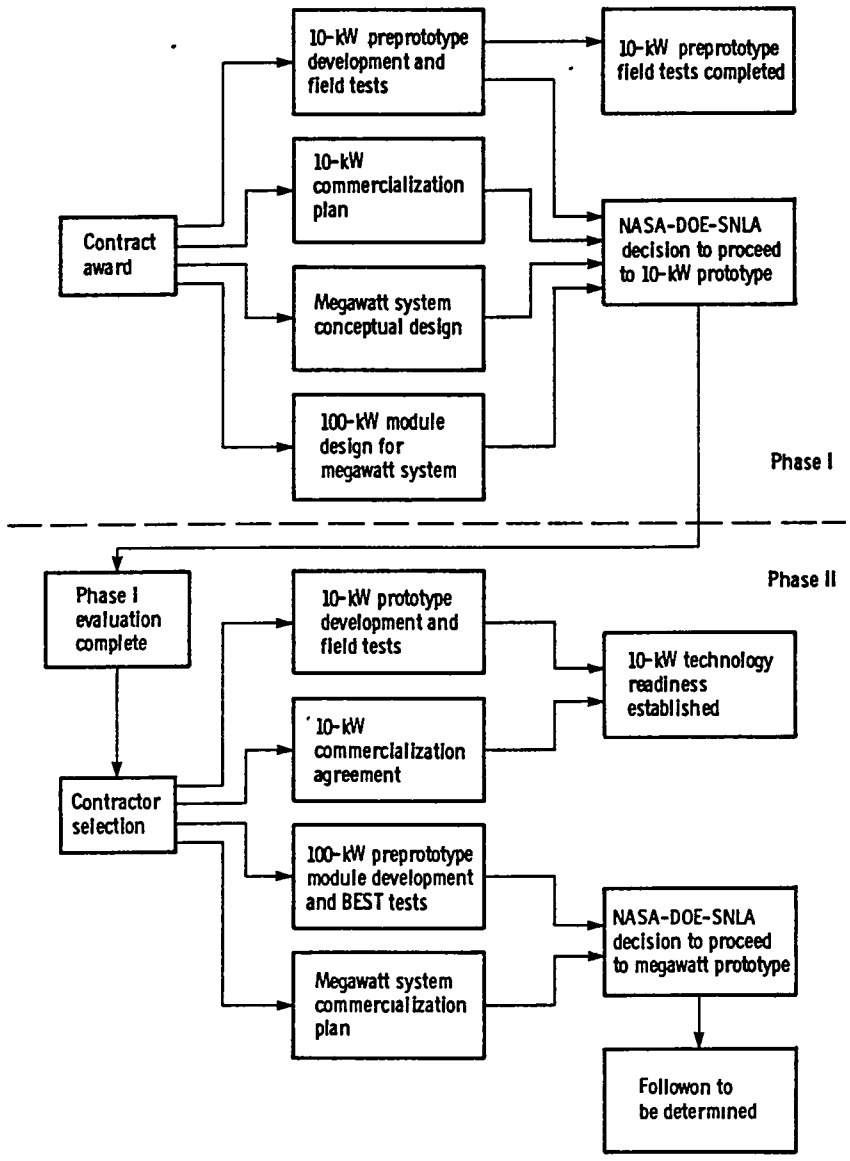

Figure 5. - Task sequence for contract activity of project element 2.0 - prototype systems development.

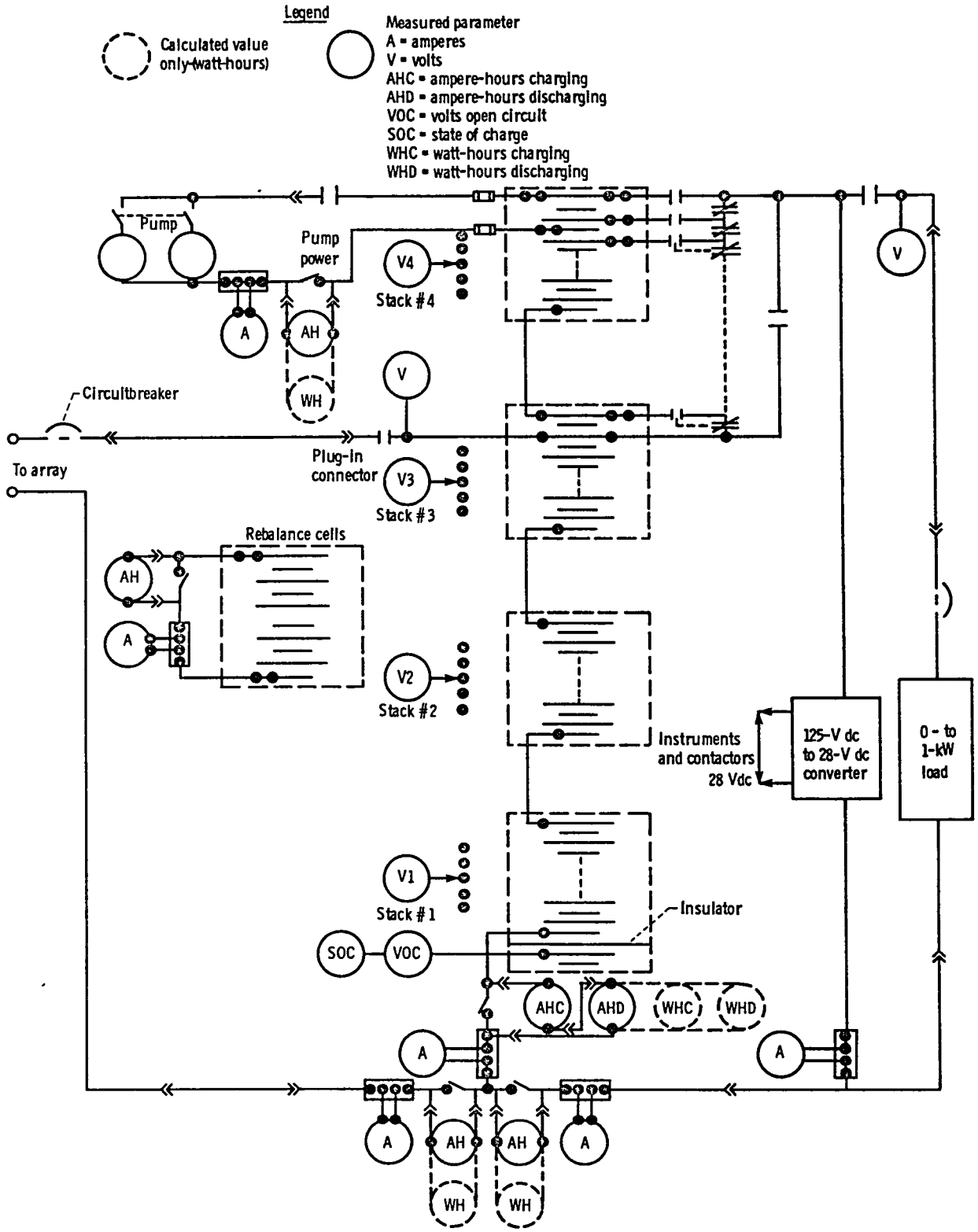

Figure 6 - Electrical schematic of NASA Lewis preprototype 1-kW Redox energy storage system

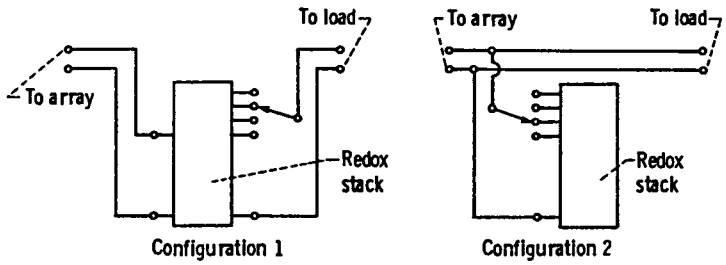

Figure 7 - Optional configurations for connection of photovoltaic array to preprototype Redox system

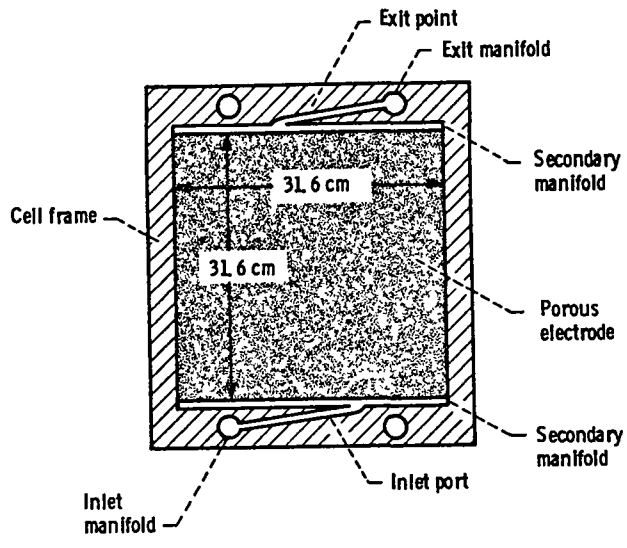

Figure 8. - Planform of Redox cell with porous carbon felt electrodes.

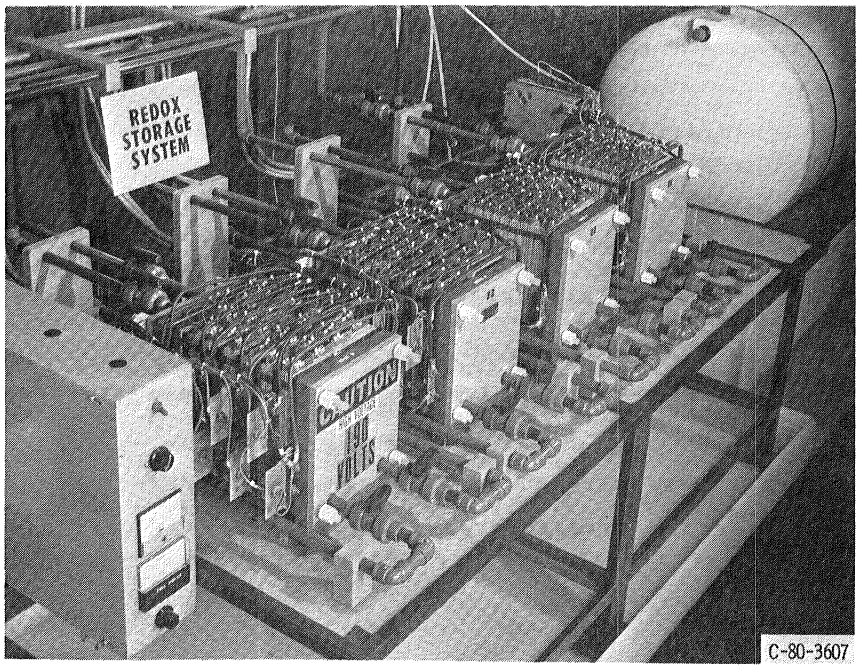

Figure 9. - NASA Lewis preprototype 1-kW Redox energy storage system.

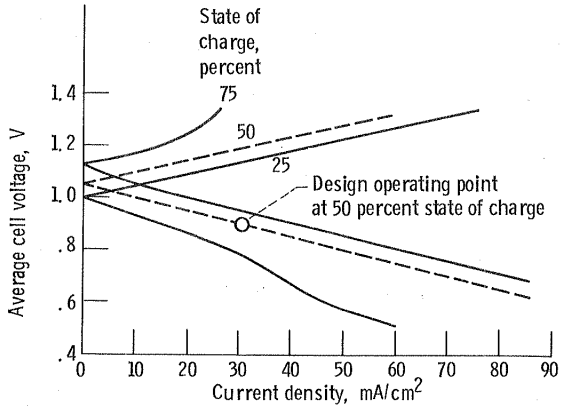

Figure 10. - Polarization curves for NASA Lewis preprototype 1-kW Redox storage system (configuration zero).

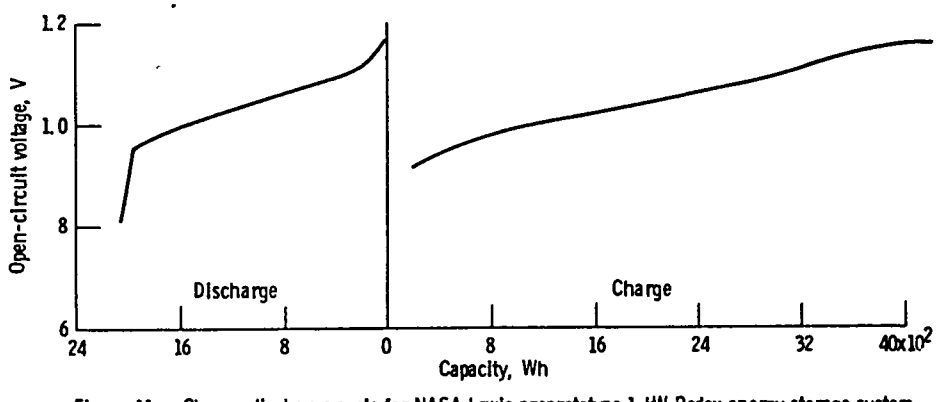

Figure 11. - Charge-discharge cycle for NASA Lewis preprototype 1-kW Redox energy storage system: charge at 12.5 A to 1.20 V/cell, then taper, discharge at 12.5 A, pump and instrument control power externally supplied (In cycling from 0.94 V to 1.15 V and back to 0.94 V, the ampere- hour efficiency was 83.9 percent and the watt-hour efficiency was 56.7 percent.)

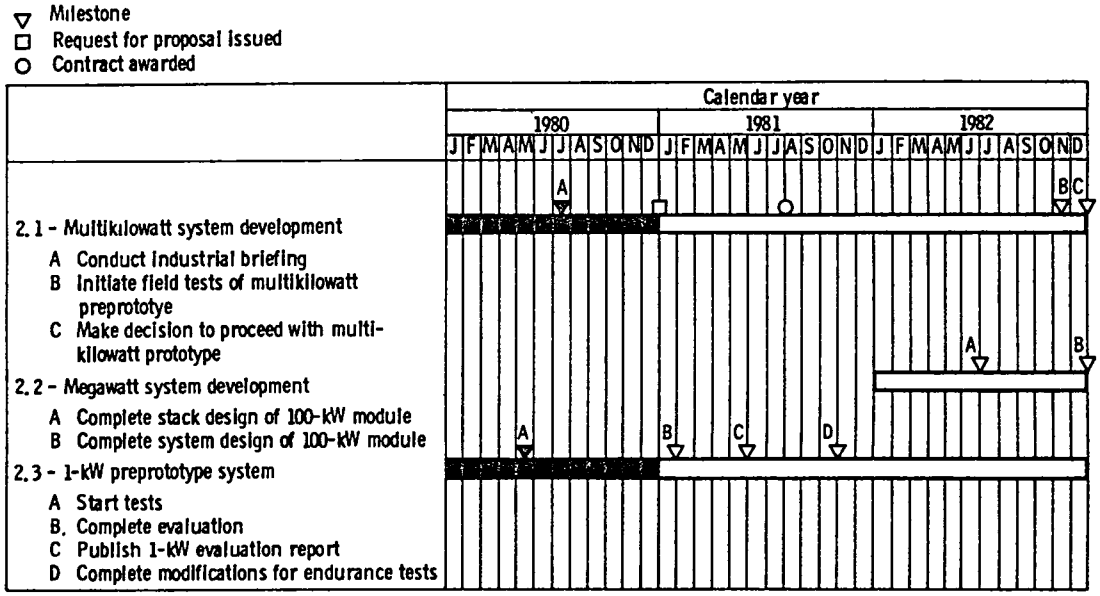

Figure 12. - Activity schedule for Redox project element 2.0 - prototype systems development.

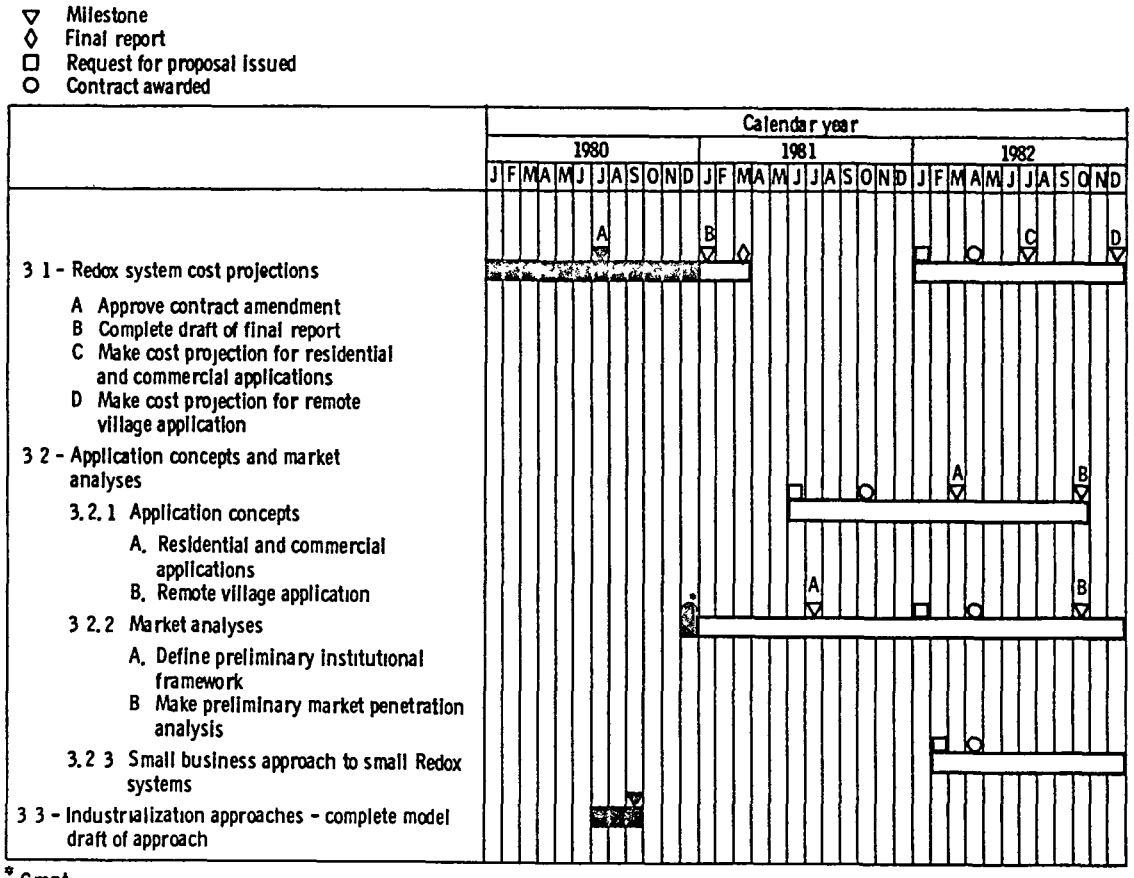

Figure 13. - Activity schedule for Redox project element 3.0 - application analyses.

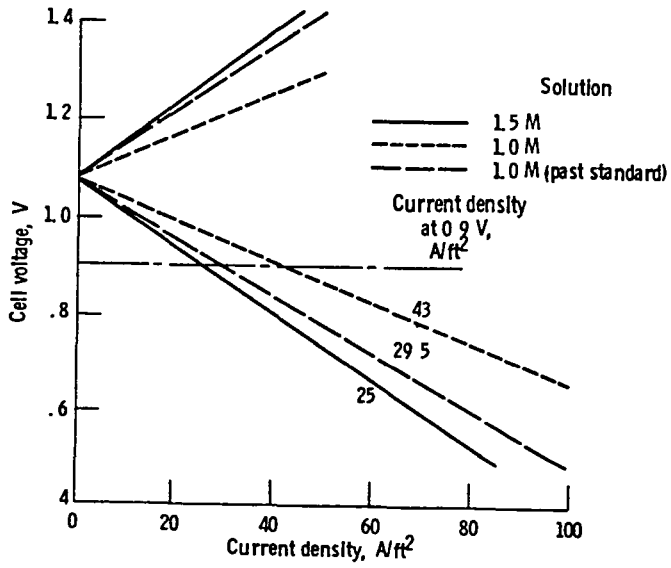

Figure 14. - Comparison of past standard cell using 1.0 molar solutions with new standard cell using 1.0 and 1.5 molar solutions

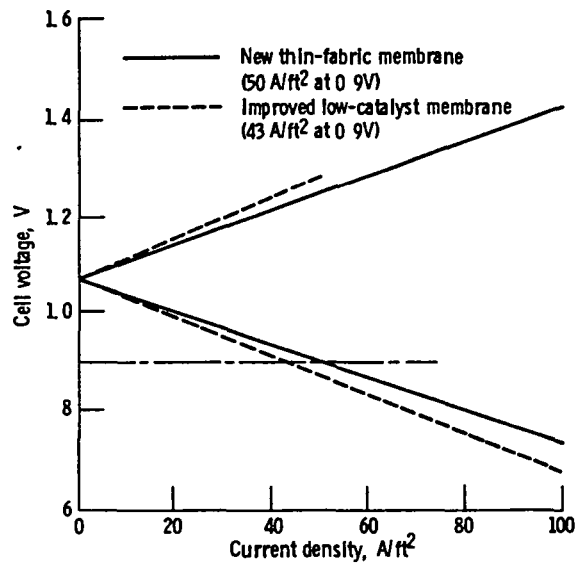

Figure 15. - Improved cell performance with new, thin-fabric membrane. Depth of discharge, 50 percent; cell area, 14.5 cm^2.

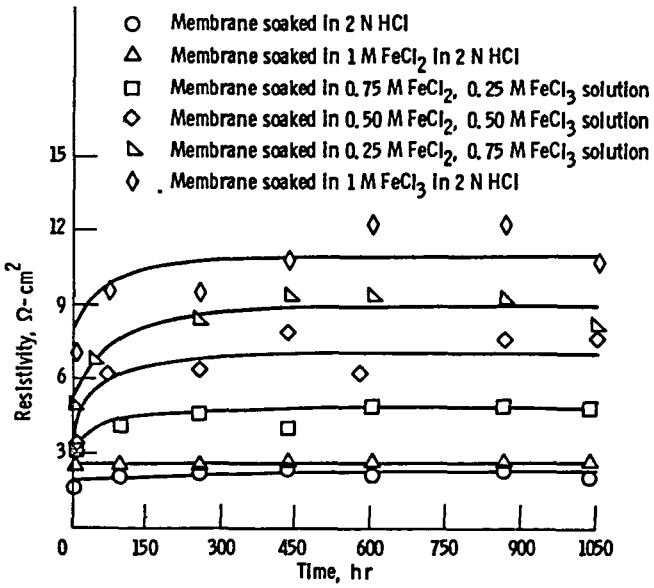

Figure 16 - Effect of Fe^{+2}/Fe^{+3} ratio on CD1L-A5-25NP area resistivity

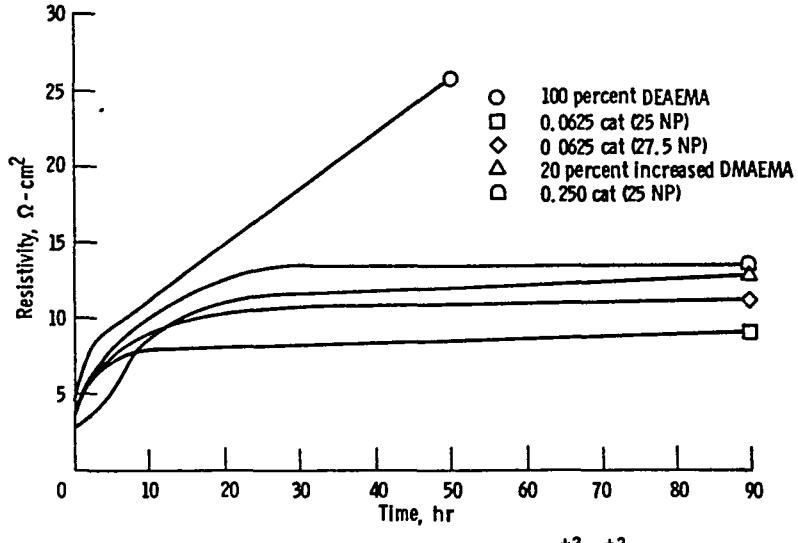

Figure 17 - Resistivities of CD1L formulations in Fe^{+3}/Fe^{+3} flow cell.

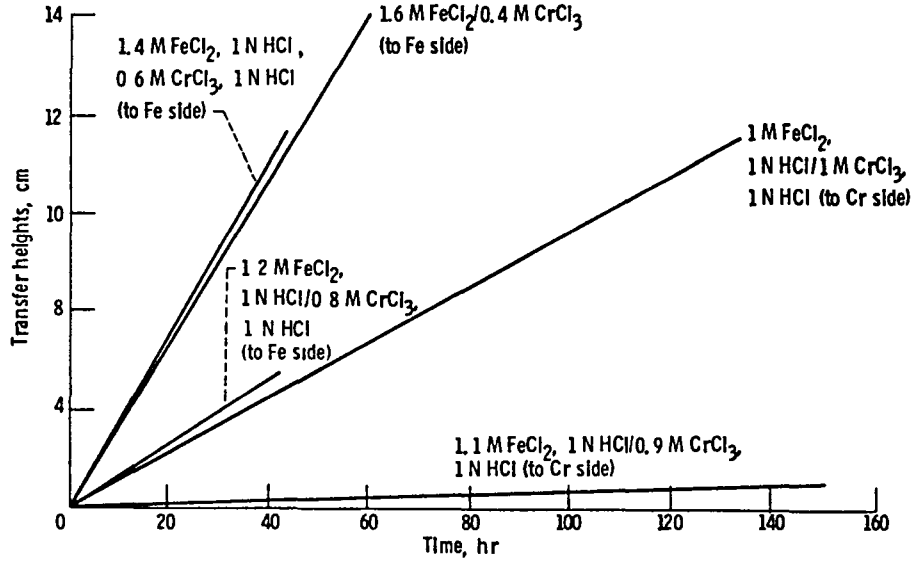

Figure 18 - Osmotic pressure tests on various discharged reactants.

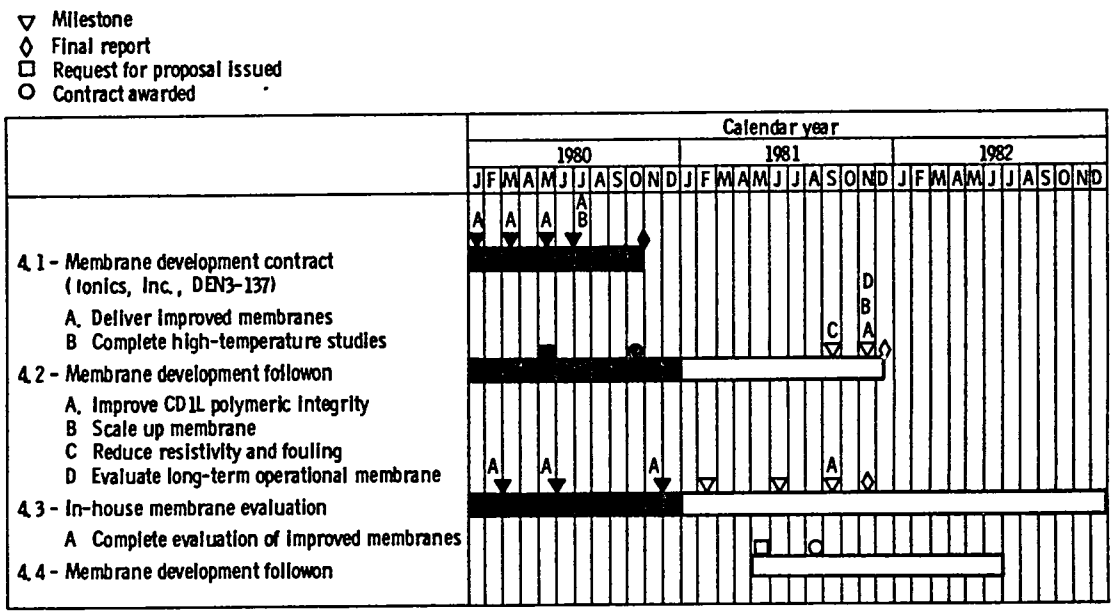

Figure 19. - Activity schedule for Redox project element 4.0 - supporting technology (membrane development).

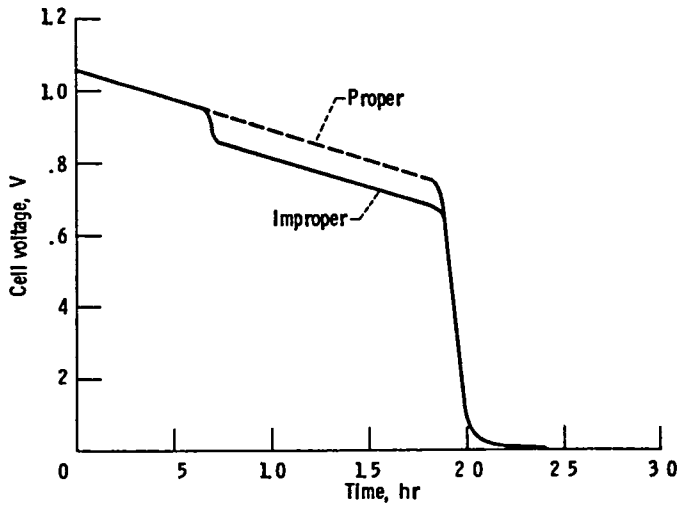

Figure 20. - Comparison of properly and improperly catalyzed chromium electrodes. Constant-current discharge.

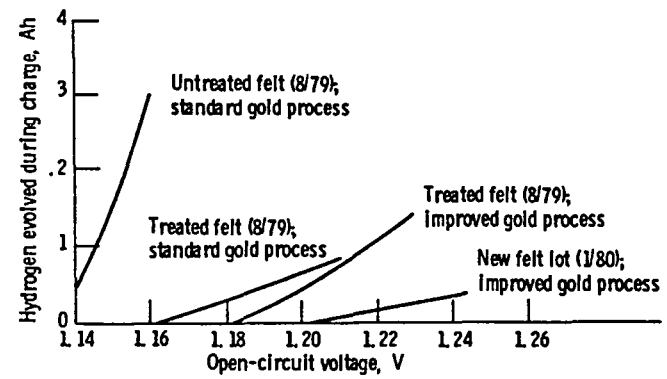

Figure 21. - Hydrogen evolution characteristics of chromium electrodes.

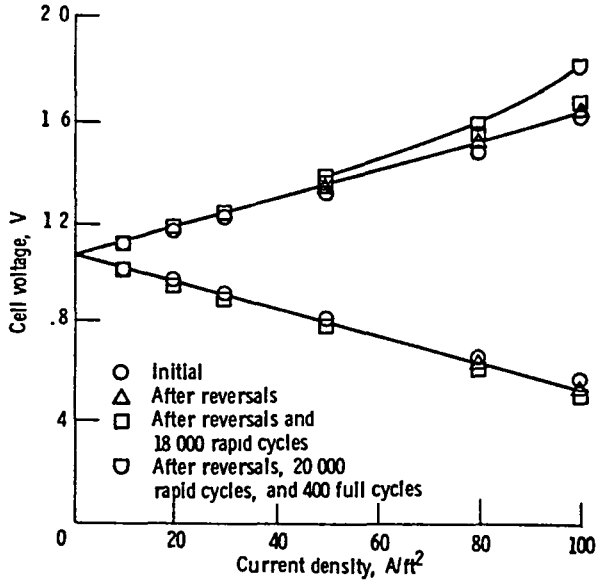

Figure 22. - Performance of 320-cm^2 single cell with optimally prepared chromium electrode Depth of discharge, 50 percent.

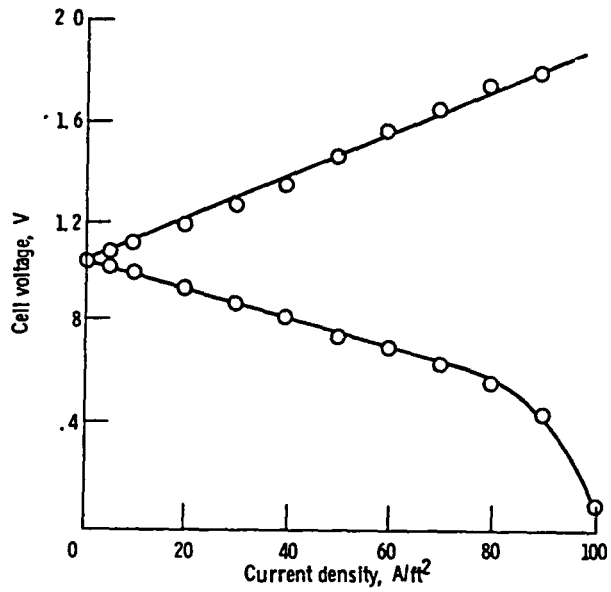

Figure 23 - Performance of planar, catalyzed chromium electrode. Depth of discharge, 50 percent; UTC carbon plate

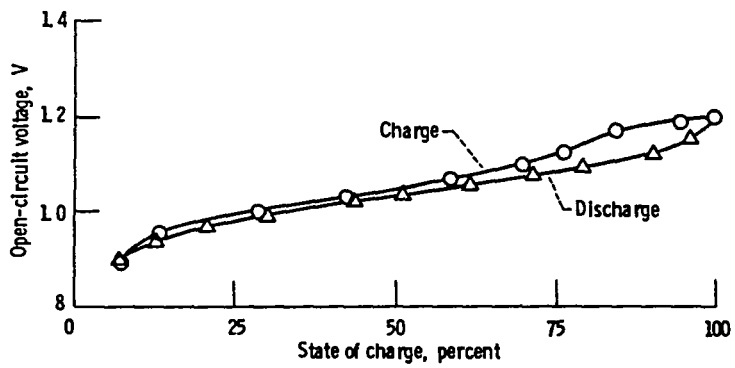

Figure 24 - Open-circuit voltage hysteresis of iron-chromium Redox cells

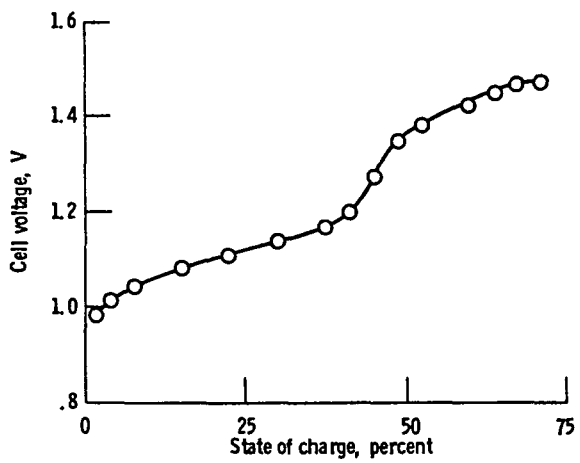

Figure 25. - Effect of chromium electrode performance on cell voltage during constant-current charge. Current, 20 mA/cm^2.

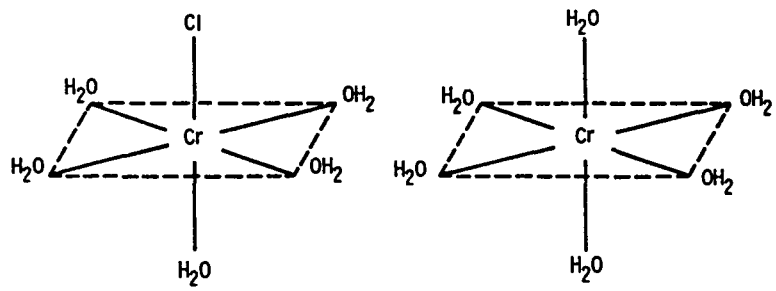

$Cr(H_2O)_5 Cl^{+2}$ — Blue-green

$Cr(H_2O)_6^{+3}$ — Blue

Figure 26. - Predominant forms of chromic ion in acidified aqueous solutions

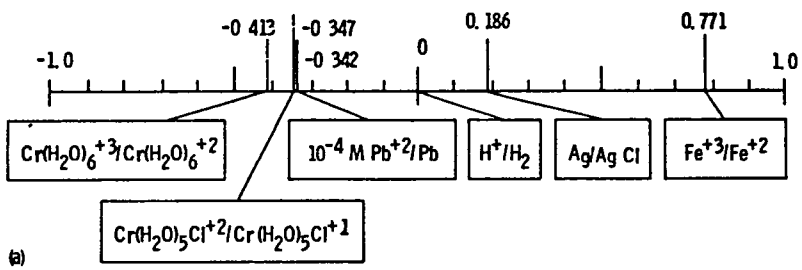

(a)

$Cr(H_2O)_6^{+3} + E^- \rightleftharpoons Cr(_2O)_6^{+2}$ 0.75×10^{-5} cm/s

$Cr(H_2O)_5 Cl^{+2} + E^- \rightleftharpoons Cr(H_2O)_5 Cl^{+1}$ 120×10^{-5} cm/s

(b) Rate of reduction of $Cr(H_2O)_5 Cl^{+2}$ is 160 times that of $Cr(H_2O)_6^{+3}$

(a) Reduction potentials versus H^+/H_2 electrode.

(b) Apparent electrochemical rate constants at equilibrium potential

Figure 27 - Thermodynamic and kinetic data for complexed chromium ions at mercury electrodes

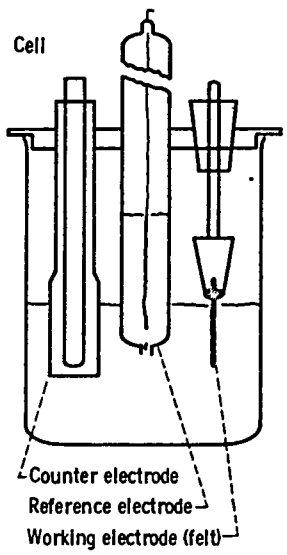

Description of experiment

Instrument passes current between working electrode and counter electrode such that the potential between working electrode and reference electrode is varied at a controlled rate. Since no current is passed through reference electrode, no polarization effects are produced here. Thus the voltage-current curve is characteristic of the working electrode only

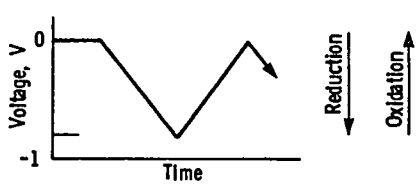

Figure 28 - Cyclic voltammetry as a tool for studying electrode phenomena

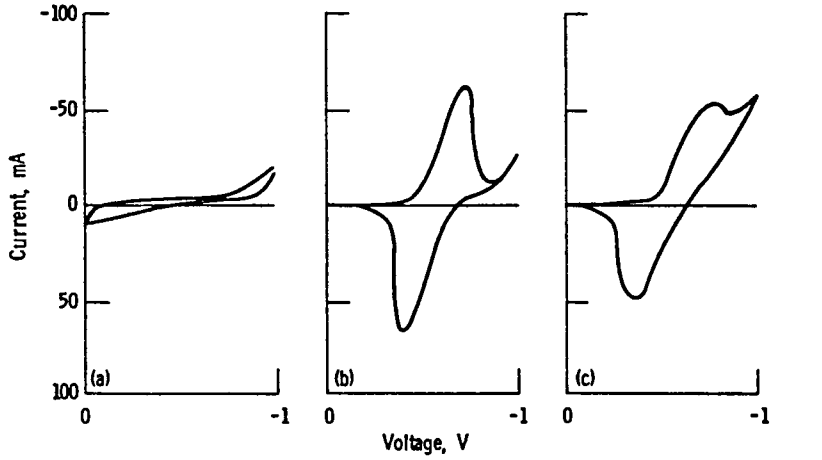

(a) Uncatalyzed felt (.05 M $CrCl_3$, 2M HCl).

(b) "Best" electrode (10^{-4} M $PbCl_2$, 2 M HCl 0.05 M $CrCl_3$)

(c) Poor electrode (good chromium activity, excessive hydrogen evolution)

Figure 29 - Cyclic voltammetry of carbon felt electrodes Scan rate, 10 mV/s; felt area, 2 cm^2, felt thickness, 0.203 to 0.229 cm, all potentials versus AgCl electrode

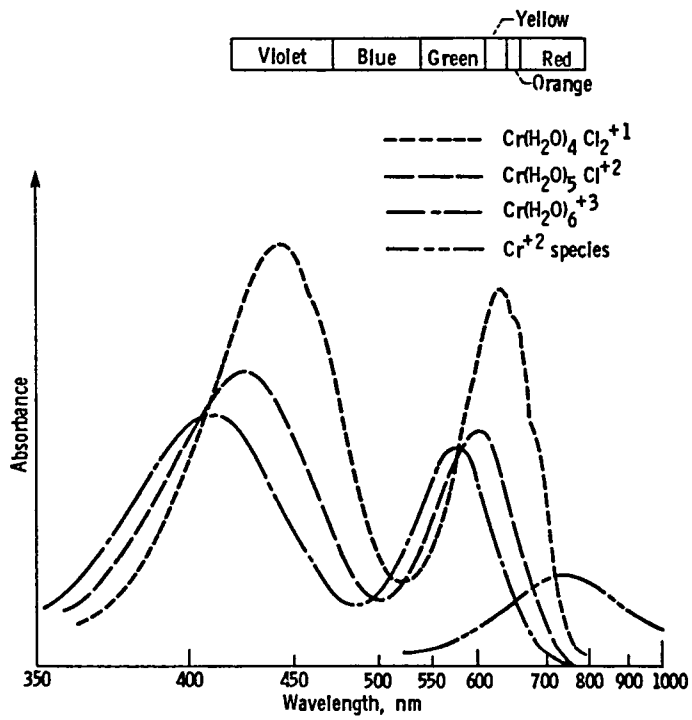

Figure 30 - Spectra of chromium complex ions

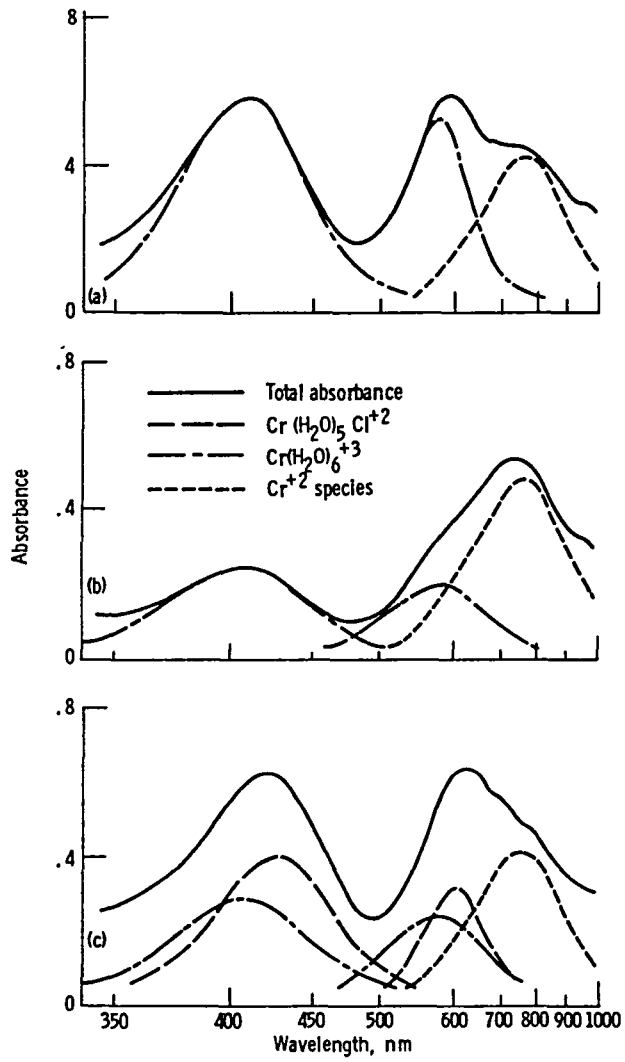

(a) During charging cycle, 71.2 percent charged
(b) At end of charging cycle, 88 3 percent charged.
(c) During discharging cycle, 69 6 percent charged

Figure 31 - Spectra of chromium Redox solutions at several states of charge

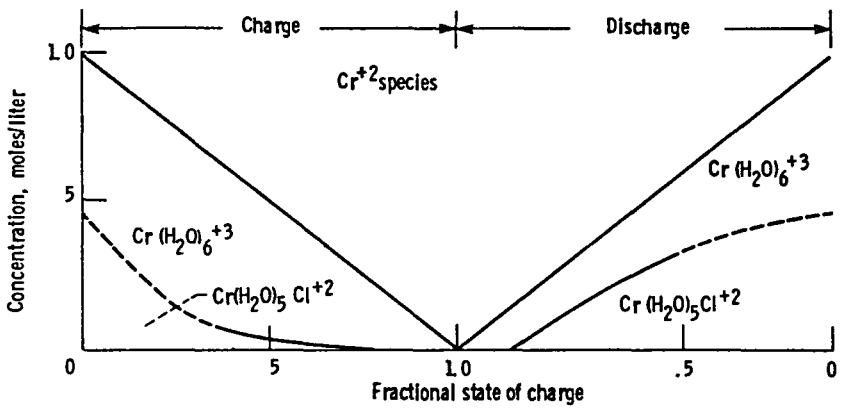

Figure 32 - Concentrations of various chromium ions during charge and discharge

▽ Milestone
◊ Final report
□ Request for proposal issued
○ Contract awarded

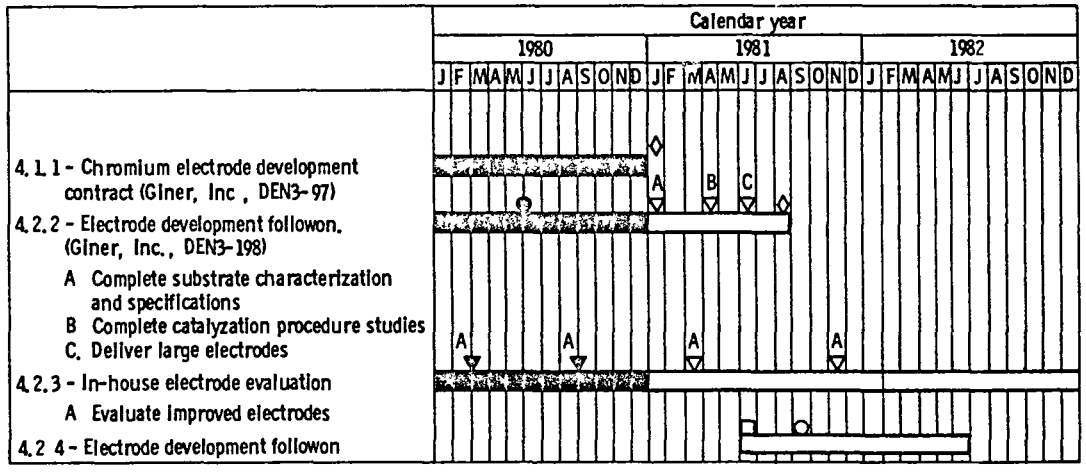

Figure 33. - Activity schedule for Redox project element 4.2 - supporting technology (electrode development).

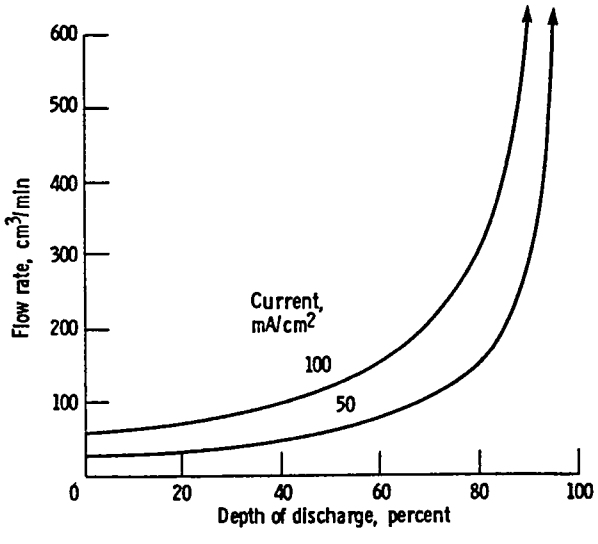

Figure 34. - Stoichiometric flow requirements for a 1000-cm^2 cell during discharge 1.0 Molar solutions

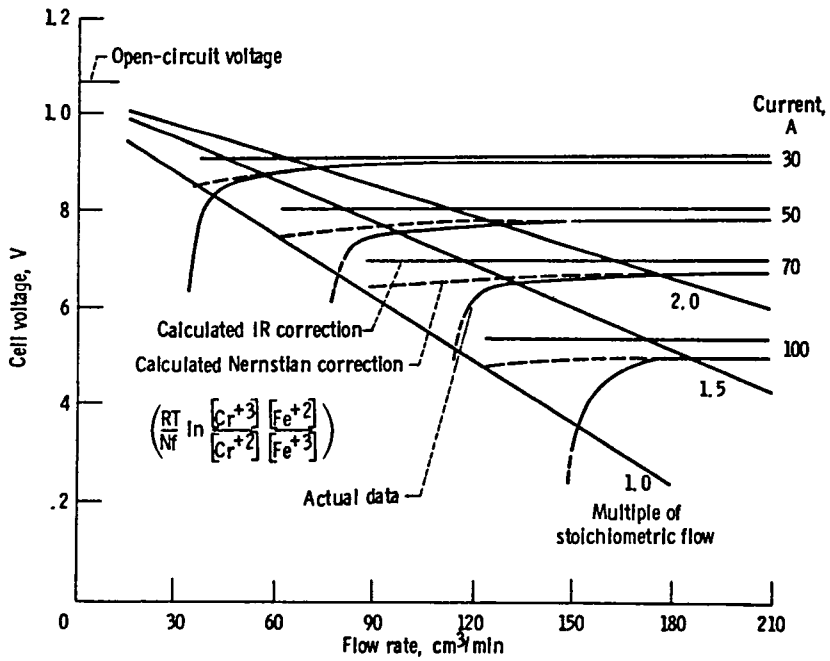

Figure 35 - Effect of reactant flow rate on single-cell performance Depth of discharge, 50 percent.

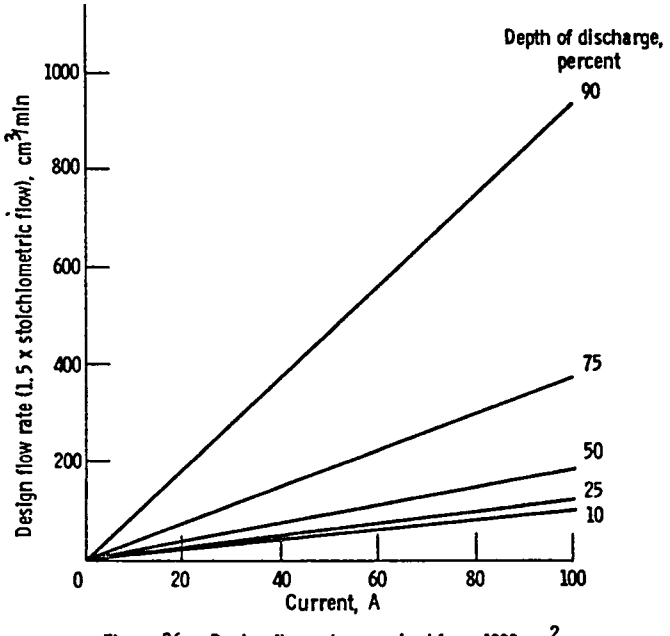

Figure 36 - Design flow rates required for a 1000-cm^2 single cell at various currents and depths of discharge. 1.0 Molar solutions.

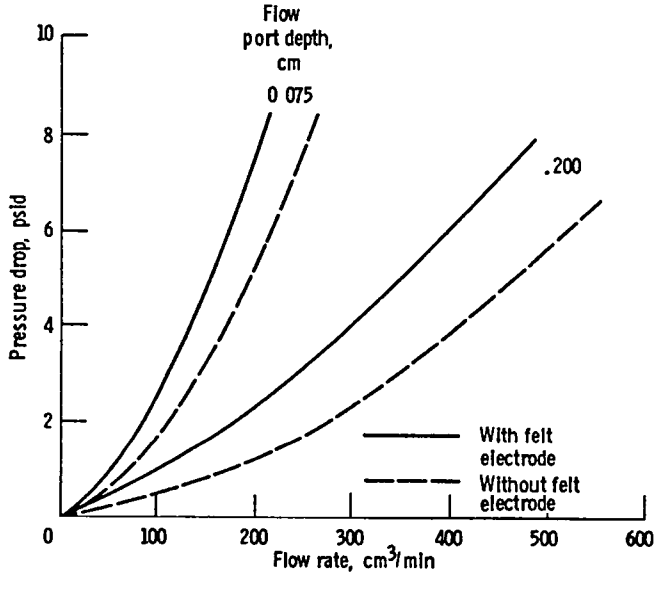

Figure 37 - Effect of flow rate on pressure drop for 1000-cm^2 cell (0.2-cm flow port width)

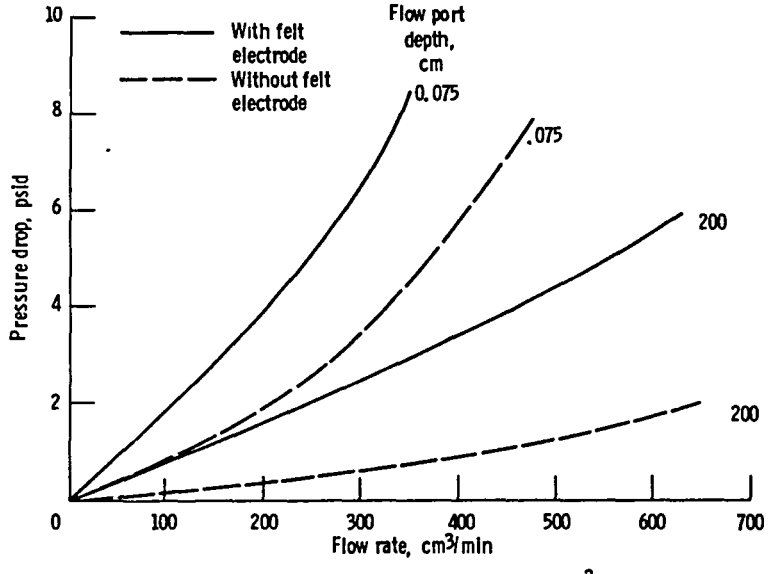

Figure 38 - Effect of flow rate on pressure drop for 1000-cm^2 cell (0.4-cm flow port width)

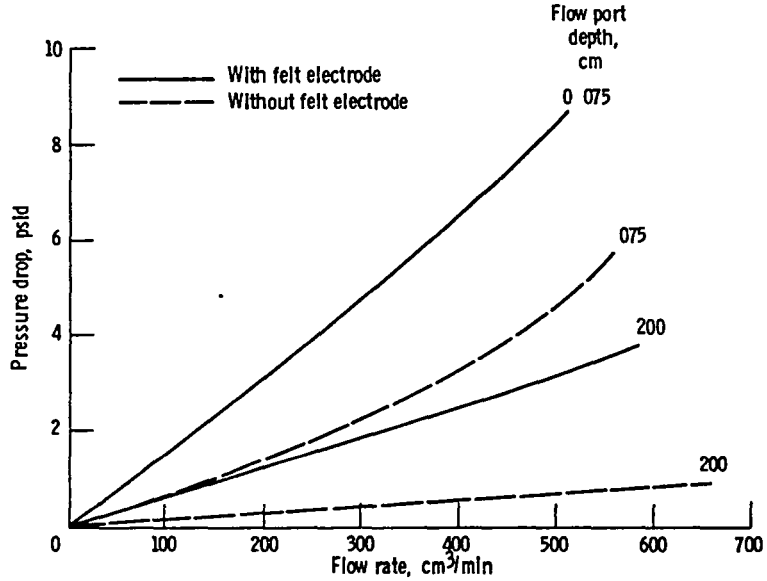

Figure 39 - Effect of flow rate on pressure drop for 1000-cm^2 cell (0.7-cm flow port width)

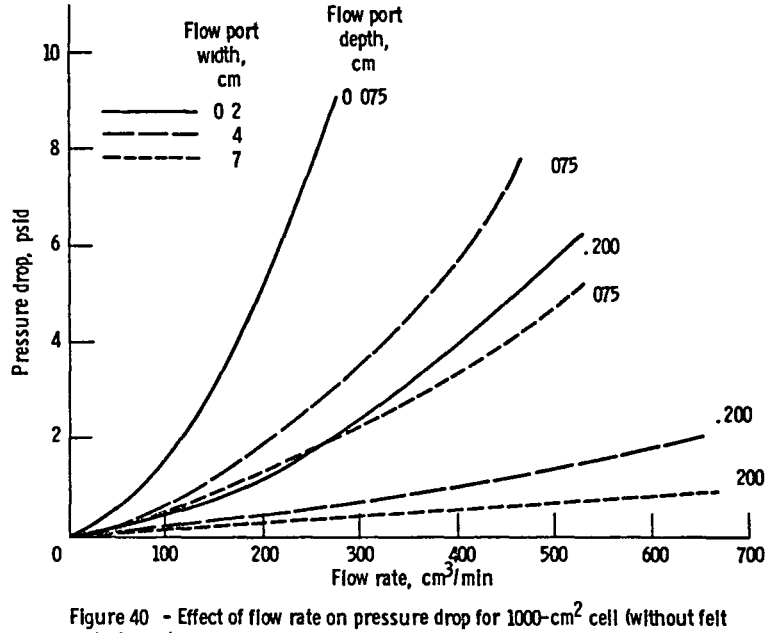

Figure 40 - Effect of flow rate on pressure drop for 1000-cm^2 cell (without felt electrodes).

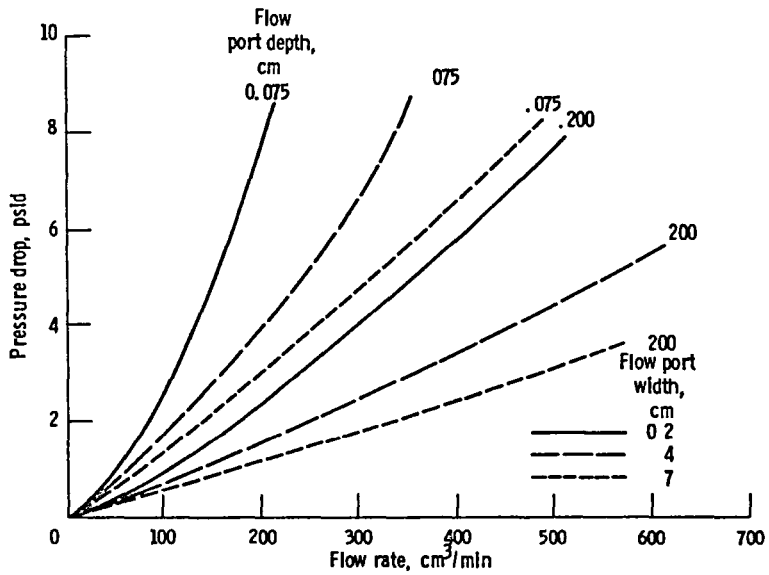

Figure 41. - Effect of flow rate on pressure drop for 1000-cm^2 cell (with felt electrodes)

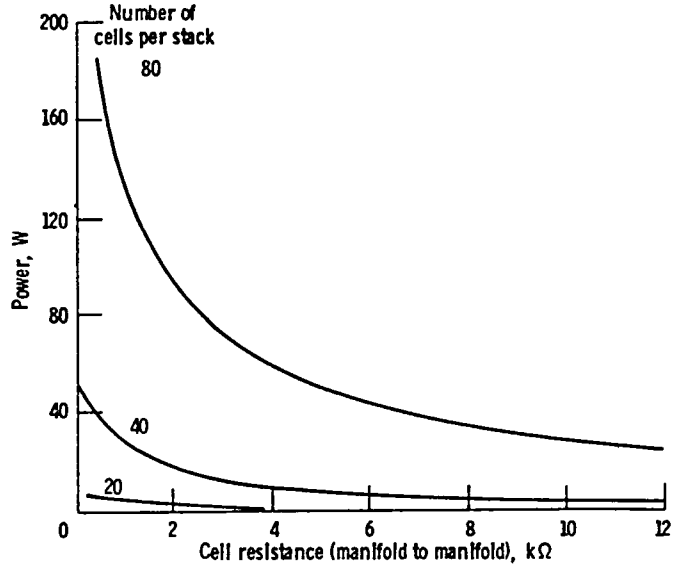

Figure 42 - Shunt-current power losses per stack, as predicted by NASA model

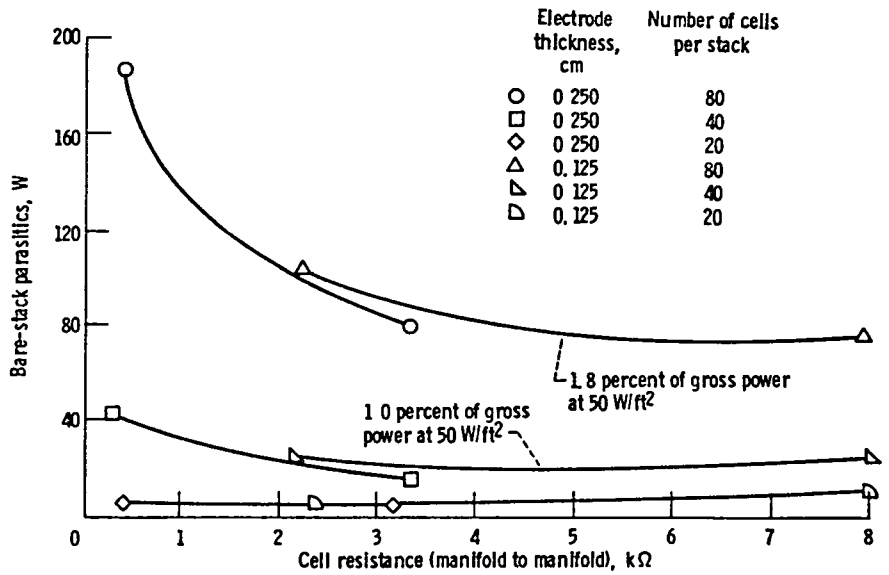

Figure 43 - Calculated sum of shunt-current power and pump power for flow cell single stacks Flow rate, 150 cm3/cell per cavity per minute, assumed pump efficiency, 60 percent.

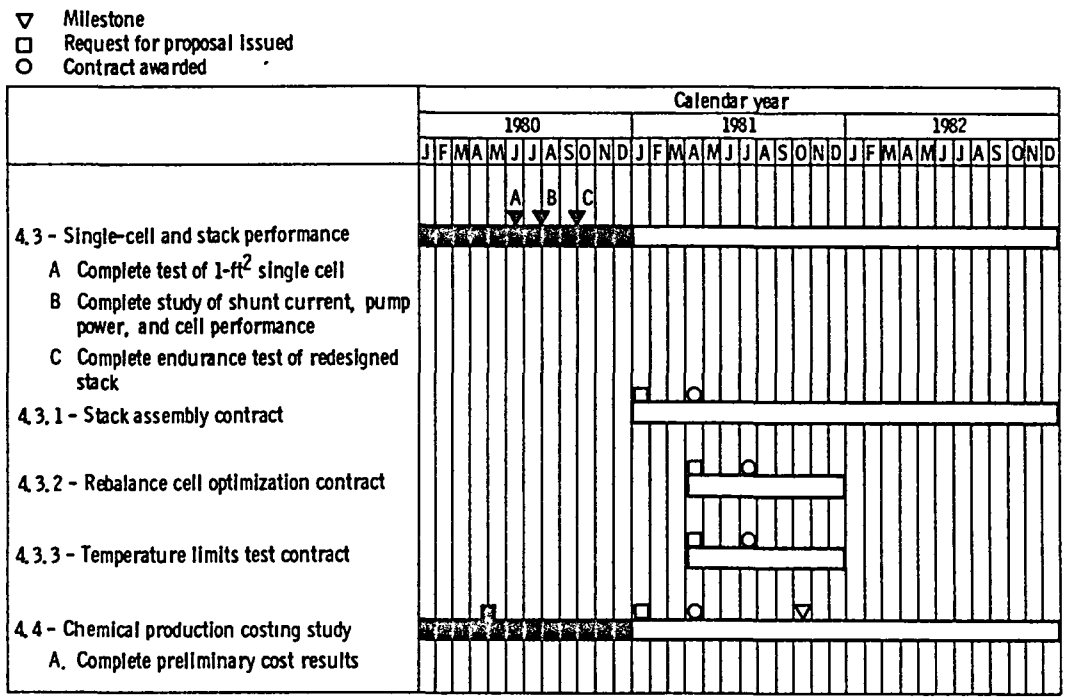

Figure 44. - Activity schedule for Redox project elements 4.3 and 4.4 - single-cell and stack performance and chemical production costing study.

1 Report No	2 Government Accession No	3 Recipient's Catalog No
NASA TM-82940		

4 Title and Subtitle	5 Report Date
NASA REDOX STORAGE SYSTEM DEVELOPMENT PROJECT Calendar Year 1980	December 1982
	6 Performing Organization Code 776-72-41
7 Author(s)	8 Performing Organization Report No E-1340
9 Performing Organization Name and Address National Aeronautics and Space Administration Lewis Research Center Cleveland, Ohio 44135	10 Work Unit No
	11 Contract or Grant No
12 Sponsoring Agency Name and Address U. S. Department of Energy Division of Energy Storage Systems Washington, D. C. 20545	13 Type of Report and Period Covered Technical Memorandum
	14 Sponsoring Agency ~~Code~~ Report No. DOE/NASA/12726-18

15 Supplementary Notes

Final report. Prepared under Interagency Agreement DE-AI04-80AL12726.

16 Abstract

The NASA Redox Storage System Development project is managed by the Redox Project Office of the Solar and Electrochemistry Division of the NASA Lewis Research Center in accordance with Interagency Agreement DE-AI04-80AL12726 (formerly DOE/NASA Agreement EC-77-A-31-1002). The Department of Energy (DOE) Headquarter's Office of Advanced Conservation Technologies has assigned lead center responsibility for this project to Sandia National Laboratories, Alburquerque, New Mexico, Storage Batteries Division of the Components and Standards Directorate. This annual report (for the period ending approx Dec. 1980) was prepared as part of the reporting requirements under this interagency agreement. The report describes the technical accomplishments pertaining to the development of Redox systems and related technology. Task elements discussed in this report are representative of DOE policies in existence during calendar year 1980.

17 Key Words (Suggested by Author(s))	18 Distribution Statement
Redox; Electrochemistry; Batteries	Unclassified - unlimited STAR Category 44 DOE Category UC-94c

19 Security Classif (of this report)	20 Security Classif (of this page)	21 No of Pages	22 Price*
Unclassified	Unclassified		

* For sale by the National Technical Information Service, Springfield, Virginia 22161

End of Document